Emergence of a recurrent insertion in the N-terminal domain of the SARS-CoV-2 spike glycoprotein

Marco Gerdol [a,*], Klevia Dishnica [b], Alejandro Giorgetti [b]

[a] *University of Trieste, Department of Life Sciences, 34127 Trieste, Italy*
[b] *University of Verona, Department of Biotechnology, 37134 Verona, Italy*

ARTICLE INFO

ABSTRACT

Tracking the evolution of the severe acute respiratory syndrome coronavirus 2 (SARS-CoV-2) through genomic surveillance programs is undoubtedly one of the key priorities in the current pandemic situation. Although the genome of SARS-CoV-2 acquires mutations at a slower rate compared with other RNA viruses, evolutionary pressures derived from the widespread circulation of SARS-CoV-2 in the human population have progressively favored the global emergence, though natural selection, of several variants of concern that carry multiple non-synonymous mutations in the spike glycoprotein. These are often placed in key sites within major antibody epitopes and may therefore confer resistance to neutralizing antibodies, leading to partial immune escape, or otherwise compensate infectivity deficits associated with other non-synonymous substitutions. As previously shown by other authors, several emerging variants carry recurrent deletion regions (RDRs) that display a partial overlap with antibody epitopes located in the spike N-terminal domain (NTD). Comparatively, very little attention had been directed towards spike insertion mutations prior to the emergence of the B.1.1.529 (omicron) lineage. This manuscript describes a single recurrent insertion region (RIR1) in the N-terminal domain of SARS-CoV-2 spike protein, characterized by at least 49 independent acquisitions of 1–8 additional codons between Val213 and Leu216 in different viral lineages. Even though RIR1 is unlikely to confer antibody escape, its association with two distinct formerly widespread lineages (A.2.5 and B.1.214.2), with the quickly spreading omicron and with other VOCs and VOIs warrants further investigation concerning its effects on spike structure and viral infectivity.

Abbreviations

ACE2	angiotensin converting enzyme 2
NTD	N-terminal domain
RBD	receptor binding domain
RBM	receptor binding motif
RGYR	radius of gyration
RIR1	recurrent insertion region 1
RMSD	root mean square deviation of backbone beads
RMSF	root mean square fluctuations
RDR	recurrent deletion region
VOC	variant of concern
VOI	variant of interest

1. Introduction

Coronaviruses generally accumulate mutations at a much lower rate than other RNA viruses, thanks to the efficient proofreading exonuclease activity exerted by nsp14, in complex the activator protein nsp10 (Denison et al., 2011; Ma et al., 2015). As a result, the rate of molecular evolution of SARS-CoV-2 is currently estimated (as of January 5th, 2022, based on GISAID data (Shu and McCauley, 2017)), to be close to 25 substitutions/year per genome, i.e. 8.36×10^{-4} substitutions/site/year, which is slightly higher than previous estimates for human endemic coronaviruses (Ren et al., 2015). Consistently with comparative genomics data obtained from other members of the *Sarbecovirus* subgenus, such mutations are not evenly distributed across the genome, but they are disproportionally located in the S gene, which encodes the spike glycoprotein. It is also worth noting that the S gene undergoes frequent recombination events, likely as a result of naturally occurring

co-infections in the animal viral reservoirs (Boni et al., 2020), and that these events are also theoretically possible among different SARS-CoV-2 lineages (VanInsberghe et al., 2021). The encoded transmembrane protein forms a homotrimer and plays a fundamental role in the interaction between the virus and host cells, promoting viral entry though the interaction with different membrane receptors (Millet et al., 2021). In the case of SARS-CoV-2 and of the closely related SARS-CoV responsible of the 2002–2004 outbreak, such receptor is represented by the angiotensin converting enzyme 2 (ACE2) (Ren et al., 2008; Walls et al., 2020).

While most of these mutations have little or no phenotypic impact at all, some may significantly influence viral transmissibility and the ability of the virus to escape host immune response. The causes underpinning such phenotypic effects may either lie in an increased viral shedding, in the alteration of the binding affinity between the spike receptor binding domain (RBD) and the host ACE2 receptor, or in the modification of key antibody epitopes. The most striking example of a non-synonymous mutation which had a dramatic impact on the dynamics of the pandemics is most certainly represented by S:D614G. This mutation, which was not present in the ancestral lineage that caused the Wuhan outbreak, emerged in the very early phases of the pandemics, quickly becoming dominant worldwide (Korber et al., 2020), most likely due to an increased packing of functional spike protein into the virion (Zhang et al., 2020).

Even though the mutation rate of the SARS-CoV-2 genome remained relatively stable throughout 2020, growing evidence soon started to point out the presence of shared mutations across multiple independent lineages, suggesting ongoing convergent evolution and possible signatures of host adaptation (van Dorp et al., 2020a). While early investigations failed to identify evidence of increased transmissibility associated with such recurrent mutations (van Dorp et al., 2020b), the nearly contemporary independent emergence of three variants sharing the non-synonymous substitution N501Y in the spike protein started to raise serious concerns about the possible involvement of this mutation in increasing viral infectivity. While the functional role of N501Y still remains to be fully elucidated, structural modeling points towards a possible function in the stabilization of the spike protein in the open conformation, which may increase ACE2 binding, especially in combination with other mutations targeting the RBD (Nelson et al., 2021; Teruel et al., 2021; Zhu et al., 2021).

B.1.1.7 (the alpha variant, according to WHO labeling), one of the emerging lineages carrying S:N501Y, spread in southeastern England in early 2020 and quickly became dominant in Europe. Despite being significantly more transmissible than wild-type genotypes (Davies et al., 2021), alpha was not associated with significant immune escape from the neutralizing activity of convalescent or vaccinated sera (Lustig et al., 2021; G.-L. Wang et al., 2021; Z. Wang et al., 2021; Xie et al., 2021). On the other hand, some point mutations present in the spike NTD, i.e. the deletion of a codon in position 144, led to full escape from the activity of a few NTD-directed monoclonal antibodies (P. Wang et al., 2021).

Two other major lineages carrying N501Y, designated as variants of concerns (VOCs) in early 2021, i.e. B.1.351 (beta) and P.1 (gamma), were linked with major outbreaks in geographical regions with very high estimated seroprevalence, i.e. in the Eastern Cape region (South Africa) (Sykes et al., 2021) and in Manaus (Amazonas, Brazil) (Sabino et al., 2021), respectively. Both variants were characterized by a constellation of non-synonymous mutations and accelerated rates of evolution, which suggested that their selection might have occurred in immunocompromised patients with persistent viral infection (Choi et al., 2020). Among the many features shared by beta and gamma, the most remarkable one was the presence of two additional RBD mutations, i.e. E484K and K417N/K417T. The former one has been identified as a key player in antibody escape, due to its presence in a major epitope recognized by class II RBD-directed antibodies (Greaney et al., 2021; Starr et al., 2020, 2021). On the other hand, mutations of K417, located in an epitope recognized by class I antibodies, are thought to provide a minor contribution to polyclonal antibody response escape (Greaney

et al., 2021) and to possibly stabilize, together with E484K and N501Y, the interaction between the RBD and the ACE2 receptor (Nelson et al., 2021). Due to the possible negative impacts of these emerging variants on ongoing vaccination campaigns (Madhi et al., 2021; Shen et al., 2021), the focus placed on molecular surveillance significantly increased throughout 2021.

In the spring of 2021, the lineage B.1.617.2 (delta) was internationally recognized as the fourth VOC. Like the three previously mentioned variants, delta carried several non-synonymous mutations in the S gene, including L452R, which is located in a major class III RBD-directed antibody epitope (Shen et al., 2021) and allows to completely escape the neutralizing activity of several monoclonal antibodies (mAbs) (Starr et al., 2021). Following its initial association with the surge of infections that occurred in India in early 2021 (Dhar et al., 2021), this variant rapidly spread worldwide and replaced alpha, which strongly suggested a higher intrinsic transmissibility (Dagpunar, 2021), possibly due to a more efficient cleavage site between the S1 and S2 subunits (Saito et al., 2021). At the same time, delta was also found to be endowed with significant immune escape properties, which resulted in reduced sensitivity towards the sera of convalescent and vaccinated individuals (Planas et al., 2021) and in reduced vaccine effectiveness, in particular after the first dose (Lopez Bernal et al., 2021). Although delta became dominant worldwide in the second half of 2021, a novel variant, designed as B.1.1.529, started to quickly spread in the Gauteng province (South Africa) in November 2021, outcompeting delta. This fitness advantage has been tentatively linked with a substantial ability to evade immunity from previous infection (Pulliam et al., 2021), which might be consistent with the high number of non-synonymous mutations and indels observed in the S gene compared with the reference SARS-CoV-2 genome. These include a number of previously described RBD mutations associated with the aforementioned VOC, such as T478K and N501Y, plus E484A, which suggested significant immune evasion properties, later confirmed by a number of in vitro studies (Cele et al., 2021; Garcia-Beltran et al., 2021; Schmidt et al., 2021; Willett et al., 2022). Based on early epidemiological data and on the growing number of imported cases reported abroad, on December 1st, 2021 WHO included B.1.1.529 in the list of VOCs under the "omicron" designation.

Several VOCs and VOIs (including alpha, beta, delta and omicron) carry spike deletions in the NTD. Such deletions were previously shown to often occur in distinct NTD sites, named Recurrent Deletion Regions (RDR), arising in different geographical backgrounds, in independent viral lineages. Some RDR sites display a significant overlap with known immune epitopes, suggesting that they may drive antibody escape (McCarthy et al., 2021). Comparatively, prior to the emergence of omicron, which carries a three amino acids-long insertion (S:ins214EPE) in the NTD of the spike protein, very little attention had been directed towards insertions. Nevertheless, such events are known to have played a fundamental role in the past evolution of SARS-CoV-2 spike protein by allowing, among the other things, the acquisition of a furin-like cleavage site, which is an uncommon feature in bat coronaviruses. This short motif, which is thought to be a key pathogenicity determinant (Johnson et al., 2021), is indeed completely absent in the closely related *Sarbecovirus* RaTG13 (Ge et al., 2016) and only partly present in the recently described RmYN02 (Zhou et al., 2020, 2021) and RacCS203 (Wacharapluesadee et al., 2021).

The present work reports the independent occurrence of at least 49 distinct insertion events at the very same NTD site, located between Val213 and Leu216, which will be hereafter referred to as Recurrent Insertion Region 1 (RIR1). The transient international spread of the RIR1 insertion-carrying lineages A.2.5 and B.1.214.2, the presence of S:ins214EPE in omicron and the identification of several insertions at this site in the alpha and delta lineages point out that more attention should be put towards the functional characterization of these codon acquisitions in the near future.

2. Materials and methods

2.1. Sequence data analysis

The global frequency of insertion and deletion mutations mapped on the SARS-CoV-2 S gene was retrieved, based on GISAID data (Shu and McCauley, 2017), from https://mendel.bii.a-star.edu.sg/ (last accessed on January 5th, 2022; credit to Raphael Tze Chuen Lee). Disruptive insertion and deletion mutations (i.e. those that interrupted the open reading frame of the S gene) and insertions carrying undetermined amino acids were discarded. Genomes carrying insertions at any position between codons 213 and 216 were grouped based on the inserted nucleotide sequence. Each group was assigned a code based on progressive Roman numerals, following their chronological order of identification; variants of the same insertion including SNPs, which were detected for insertion III, IV and XLI, were disregarded. The nucleotide sequences of representative entries for each of the identified insertions were aligned with the Wuhan-Hu-1 isolate SARS-CoV-2 reference sequence (GenBank ID: NC_045512.2) using MUSCLE (Edgar, 2004) in the MEGA X environment (Kumar et al., 2018), initially preserving codon boundaries. The multiple sequence alignment was then manually refined to reflect the most probable location of the insertion within each codon. Each event was consequently classified as a phase 0, phase I or phase II insertion, annotating insertions with ambiguous placement.

All SARS-CoV-2 genome data used for phylogenetic inference in this study were retrieved from GISAID (Shu and McCauley, 2017). In detail, all available sequenced genomes belonging to the lineage A.2.5, to the related sublineages A.2.5.1, A.2.5.2 and A.2.5.3, and to the sister lineage A.2.4 were downloaded, along with associated metadata. While all available GISAID entries were considered for reporting observation frequencies, only high quality genomes (i.e. those listed as "complete" and "high coverage") associated with a sampling date were taken into account for further analysis. Genomes containing long stretches of Ns (i. e. comprising more than 25 consecutive undetermined nucleotides) were discarded. The reference isolate Wuhan-Hu-1 was also included for tree rooting purposes. Note that several genome sequences from Panama with sampling date anterior to November 2021 were disregarded due to the unreliability of associated metadata (i.e. the sampling dates appeared to be inconsistent with the very small genetic distances with recent isolates belonging to the same lineage). Overall, the A.2.5-focused datasets included 1283 sequences.

SARS-CoV-2 genomes were analyzed with the nextstrain *augur* pipeline (https://github.com/nextstrain/augur). Briefly, nucleotide sequences were aligned with MAFFT (Katoh et al., 2002) and the resulting multiple sequence alignment was used as an input for a maximum likelihood phylogenetic inference analysis, carried out with FastTree (Price et al., 2010) under a generalized time reversible model of molecular evolution. The resulting tree was further refined in the *augur* environment with treetime v.0.8.1 (Sagulenko et al., 2018) using sampling date metadata, generating a time-calibrated tree. The phylogenetic tree was rooted based on the oldest available genotype, which in this case was Wuhan-Hu-1, and graphically rendered using FigTree v.1.1.4.

A root-to-tip genetic distance analysis was performed by plotting the sampling dates against the total number of nucleotide substitutions (excluding insertions and deletions) observed in genomes belonging to the A.2.5 lineage and related sublineages. These were calculated with MEGA X (Kumar et al., 2018), compared with the reference genotype Wuhan-Hu-1. The global average genome-wide mutation rate of SARS-CoV-2, roughly equivalent to 25 substitutions per year, was retrieved from GISAID (as of January 5th, 2022).

2.2. System setup of coarse-grained models

The simulations on the wild-type spike protein were carried out considering the crystallographic structure deposited in PDB (accession ID: 6XR8) (Cai et al., 2020). A few missing portions were modeled with Swiss Model (Waterhouse et al., 2018) in order not to compromise the molecular dynamic properties of the protein. Homology modeling was performed to obtain the 3D structure of the spike protein of A.2.5 with Swiss Model (Waterhouse et al., 2018), using the EPI_ISL_1,502,836 GISAID entry as a reference. The protein structure was converted to a coarse-grained Martini representation using the martinize.py script (Aguayo-Ortiz et al., 2017). The coarse-grained protein coordinates were then positioned in the center of a simulation box of size $23 \times 23 \times 23$ nm^3.

The Martini coarse-grained force field with an Elastic Network (CG-ElNeDyn) (Aguayo-Ortiz et al., 2017) was used for running the molecular dynamics simulations through the Gromacs 2019.3 package (Van Der Spoel et al., 2005). The analyses were run using isothermal-isobaric NPT ensemble equilibrium simulations. The temperature for each group (protein, water and ions) was kept constant at 315 K using V-rescale thermostat (Bussi et al., 2007) with a coupling constant of 1.0 ps. The pressure was isotropically controlled by a Parrinello-Rahman barostat (Martonák et al., 2003) at a reference of 1 bar with a coupling constant of 12.0 ps and compressibility of 3×10^{-4}. Non-bonded interactions were used in their shifted form with electrostatic interactions shifted to zero in the range of 0–1.1 nm. A time step of 20 fs was used with neighbor lists updated every 20 steps. Periodic boundary conditions were used in the x, y and z axes. ~4μs were collected for the simulations of the wild type and mutant (i.e. A.2.5) spike proteins, respectively. The root mean square deviation of backbone beads (RMSD), the root mean square fluctuations (RMSF) and the radius of gyration (RGYR) were calculated using the gmx rms, rmsf and gyrate modules from the Gromacs package (Van Der Spoel et al., 2005). Principal component analysis (PCA), computed with MDAnalysis, was restricted to backbone beads, as it is less perturbed by statistical noise and provides significant characterization of the essential space motions (Michaud-Agrawal et al., 2011). To visualize the direction and extent of the principal motions of the simulated systems, a porcupine plot analysis was performed using the modevectors.py script in Pymol (DeLano, 2002).

3. Results and discussion

3.1. Presence of a recurrent insertion region (RIR1) in the N-terminal domain of SARS-CoV-2 spike protein

The analysis of the genomic data deposited in GISAID revealed that, before the emergence of omicron in November 2021, S gene insertions (excluding those that disrupted the open reading frame) were present in just a minor fraction of all sequenced SARS-CoV-2 genomes, i.e. roughly 0.3% of the total. Overall, the frequency of observation of spike deletions was more than 500 folds higher than spike insertions, even though this ratio is now rapidly changing due to the spread of omicron. As previously reported by other authors, most deletions occur in specific sites of the N-terminal domain, including the four previously identified Recurrent Deletion Regions (RDR) 1, 2, 3 and 4, associated with several widespread VOCs and VOIs (**Fig. 1**) (McCarthy et al., 2021), and the deletion which characterizes the delta variant, occurring at positions 157/158. This is consistent with the higher rate of mutation observed for the S1 region (which includes the NTD and RBD) in human coronaviruses compared with the more slowly evolving S2 subunit (Kistler and Bedford, 2021).

Despite their lower frequency of observation, insertions do not occur randomly in the S gene. In fact, the overwhelming majority of the insertion mutations mapped so far in SARS-CoV-2 S gene target the NTD, being in most cases identified at a specific site, located between codons 213 and 216 (**Fig. 1**). However, this figure might be an underestimate due to the frequent use of reference-based insertion-unaware algorithms for SARS-CoV-2 genome assembly, especially during the early phases of the pandemics. Due to the convergent finding of such insertions in independent viral lineages (see below), this region will be hereafter named Recurrent Insertion Region 1 (RIR1).
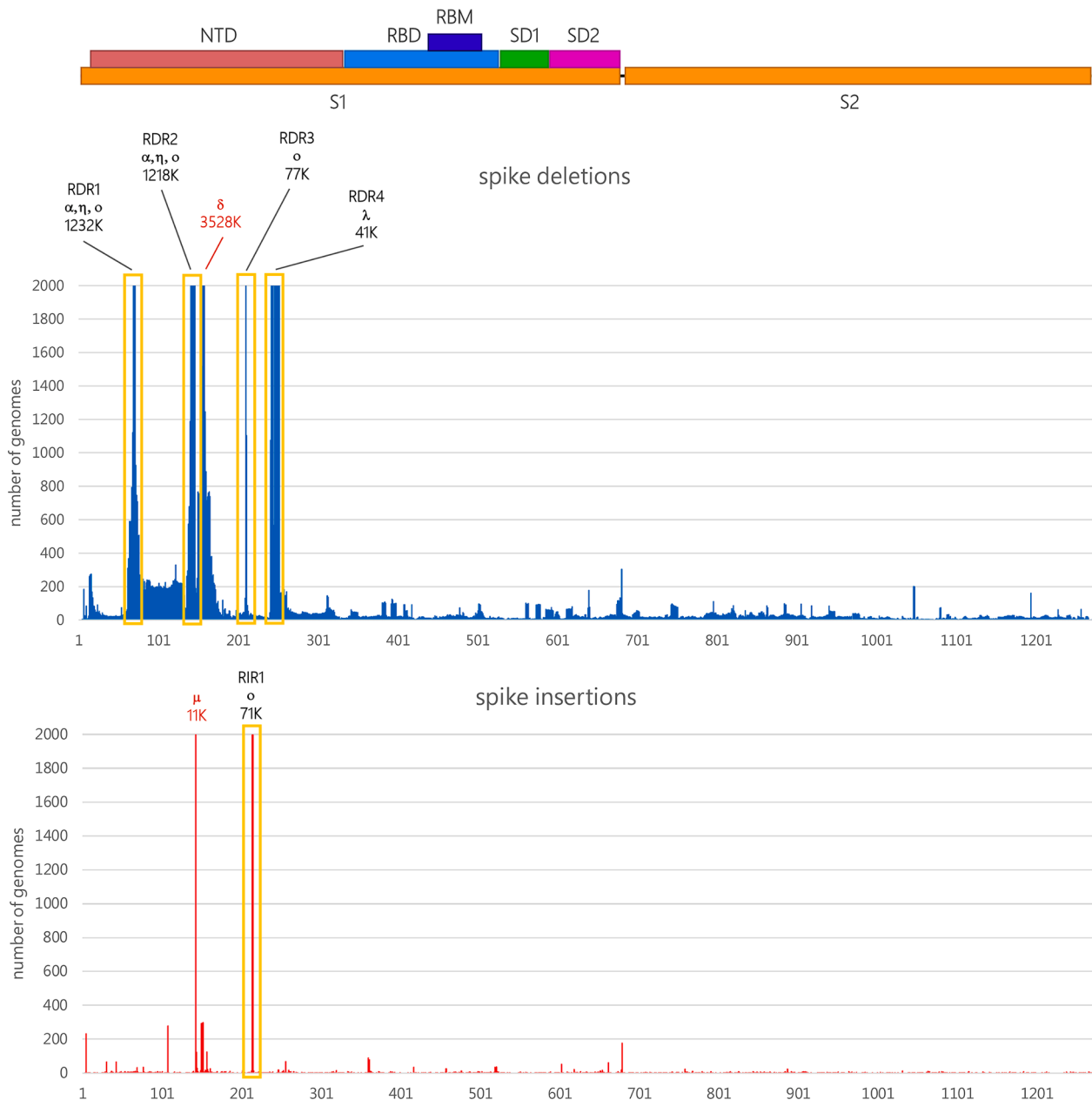
Fig. 1. Schematic representation of the SARS-CoV-2 protein, with indication of the two functional S1 and S2 subunits, which are separated by a furin-like proteolytic cleavage site, the N-terminal domain (NTD), the receptor binding domain (RBD) and receptor binding motif (RBM), the SD1 and SD2 subdomains. The absolute number of observed deletion mutations along the S-gene are reported (https://mendel.bii.a-star.edu.sg/ was last accessed on January 5th, 2022). Bars were truncated at 2000 observed genomes; in such cases, the approximate absolute number of observations is reported above the truncated bars, together with the main VOCs and VOIs associated with each indel, indicated with a Greek alphabet letter. The position of RDR1-RDR4 from a previous study (McCarthy et al., 2021), as well as the deletion 157/158 characterizing the delta variant and the ins145T insertion characterizing the mu variant, are reported.

Even though insertions were observed at several other spike sites, RIR1 was the only one where multiple insertions have independently occurred in different lineages. The only other spike insertions site with more than 1000 occurrences among the sequenced SARS-CoV-2 genomes (as of January 5th, 2022) is ins145T, found in the VOI mu (Laiton-Donato et al., 2021) (Fig. 1).

3.2. RIR1 insertions independently emerged in multiple viral lineages

As of January 5th, 2022 RIR1 insertions could be documented as the result of at least 49 independent events that occurred in different branches of the SARS-CoV-2 phylogenetic tree, which strongly suggests convergent evolution. Even though the length of the insertion spanned

from one to eight codons (Fig. 2), the overwhelming majority of the genomes with RIR1 insertions only included three codons (Table 1).

The most prominent viral variant carrying an insertion at RIR1 (the XLI 215:EPE insertion, see Table 1) is undoubtedly the emerging VOC omicron (which includes the lineages B.1.1.529, BA.1, BA.2 and BA.3), which, as of January 5th, 2022, is rapidly outcompeting delta worldwide. Although omicron was first detected on November 8th, 2021, time-calibrated Bayesian phylogenetic analyses suggest that it might have been spreading undetected in Southern Africa since early October (Viana et al., 2021). The XLI insertion is paired with three small deletions in the spike NTD: (i) Δ69/70 at RDR1, which has been previously suggested to act as a "permissive" mutation to compensate otherwise slightly deleterious immune escape mutations (Meng et al., 2021); (ii)
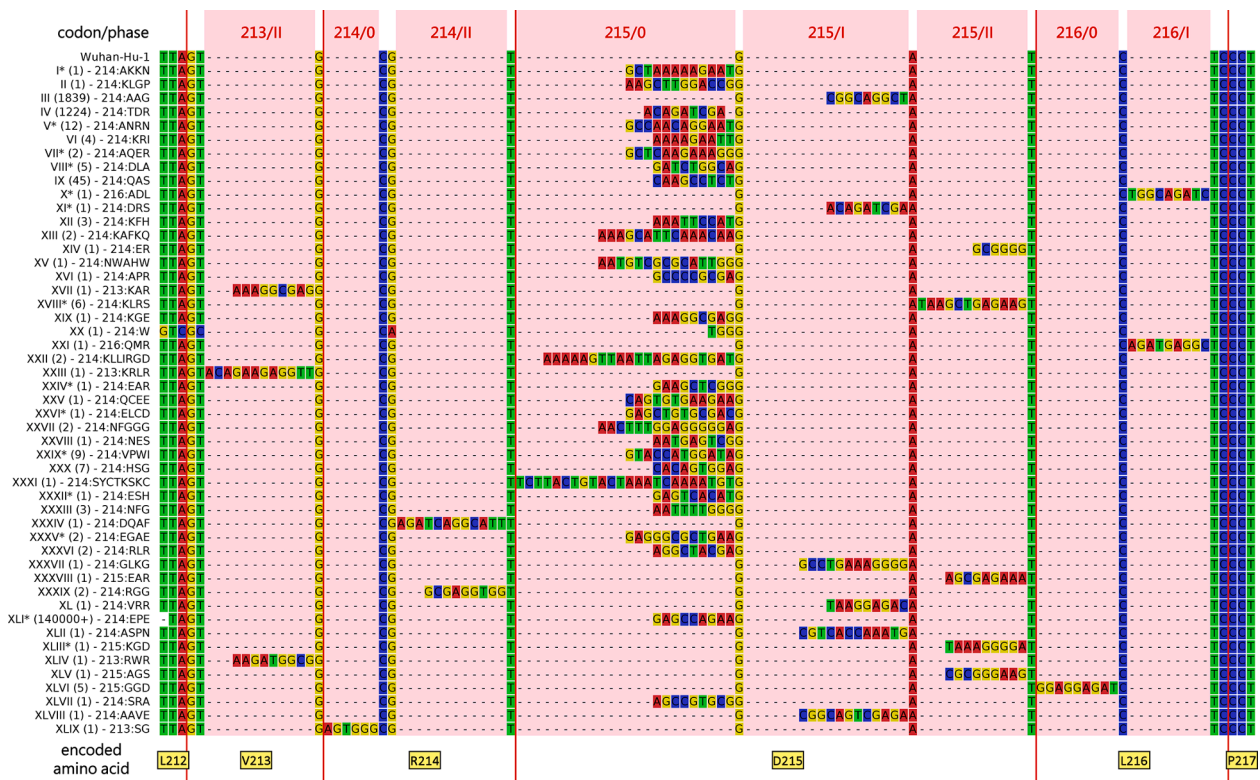
Fig. 2. Multiple sequence alignment of the nucleotide sequences of the SARS-CoV-2 S gene of the viral lineages characterized by an insertion at RIR1, compared with the reference sequence Wuhan Hu-1. The multiple sequence alignment only displays a small portion of the S gene and of the encoded spike protein, zoomed-in and centered on RIR1 (i.e. codons 212–217). Red vertical bars indicate codon boundaries, with the encoded amino acids (in the Wuhan Hu-1 reference sequence) indicated below. The number of observed GISAID entries for each insertion as well as the encoded amino acid sequences are shown near the insertion name. Please note that the exact position of all insertion could not be unambiguously detected in all cases; those with ambiguous placement are marked with an asterisk (see **Table 1** for details).

Δ143/144/145 at RDR2, known to fall within a relevant antibody epitope (McCarthy et al., 2021); (iii) Δ212, with unknown functional significance, located close to the RIR1 site. In addition, omicron carries an unprecedented number of non-synonymous mutations in the S1 subunit, some of which had been previously described in other VOCs and VOIs and linked either with antibody escape, improved ACE2 binding or proteolytic cleavage. For example, these mutations include E484A, N501Y and P681H: the first one involves a residue also mutated in beta, gamma and mu (E484K), which plays a major role in polyclonal sera escape (Harvey et al., 2021). The second one is shared by alpha, beta, gamma and mu, and may increase ACE2 binding (Nelson et al., 2021; Teruel et al., 2021; Zhu et al., 2021). The third one, shared with alpha and mu, involves a residue mutated also in delta, where the substitution of proline with arginine dramatically enhances spike cleavage and viral fusogenicity (Saito et al., 2021).

This unusual pattern of mutations results in significant immune escape in vitro and in an enhanced reinfection potential in vivo (Cele et al., 2021; Garcia-Beltran et al., 2021; Schmidt et al., 2021; Willett et al., 2022). Moreover, omicron displays an altered cellular tropism and cell entry mechanism, which depend on the acquisition of an enhanced ability to rely on the TMPRSS2-independent endosomal route (Peacock et al., 2022; Willett et al., 2022). It is presently unclear whether and to which extent the XLI insertion provides a contribution to the unique biological properties of this variant.

Unlike omicron, most RIR1 insertions were associated with very small local clusters that did not lead to further spread. However, the lineages A.2.5 (insertion III) and B.1.214.2 (insertion IV) were associated with a significant community spread (**Table I**), reaching high prevalence in some geographical regions during 2021. While A.2.5 will be discussed in detail as a case study in the following section, it is worth

briefly reporting here the transient spread of B.1.214.2. Following an initial importation from central Africa to Europe in late 2020, this lineage accounted for a non-negligible fraction of the covid-19 cases recorded in Belgium and Switzerland between March and April 2021. The spread of B.1.214.2, which led to over 1000 documented infections worldwide, was followed by a significant drop in its frequency of observation, which occurred in parallel with the rise of alpha, and further declined when delta became dominant. This lineage has not been detected since early July 2021 and can be thus provisionally considered as extinct. Insertion IV, which results in the addition of the TDR tri-peptide between R214 and D215, was associated with the presence of two other non-synonymous spike mutations located on the RBD (i.e. Q414K and N450K). These have been previously linked with a moderate increase in RBD stability (Teng et al., 2021) and with immune escape both towards a few mAbs and towards convalescent sera (Liu et al., 2021), respectively. Due to the lack of functional data, it is presently unknown whether insertion IV and the other aforementioned mutations endowed this lineage with improved transmissibility or with increased potential for reinfection.

Several other insertion events at RIR1 occurred in lineages identified as VOCs or VOIs by WHO, CDC, ECDC or PHE, including some that have been recently de-escalated to the status of variants under monitoring. In detail, insertion V was found in twelve viral genomes belonging to the gamma lineage, sequenced in different Brazilian states and Guyana between December 2020 and April 2021, indicating the presence of community transmission in the region. As reported in a previous work (Resende et al., 2021), these genomes belong to a monophyletic P.1-like clade that appears to be basal to P.1. The highly transmissible alpha lineage, which became dominant in Europe and quickly spread worldwide in early 2021 (Volz et al., 2021), before the rise of delta, was

Table 1
Summary of the 49 independent RIR1 insertions found in the SARS-CoV-2 genome, ordered by the earliest date of detection, as of January 5th, 2022.

Designation	Insertion	Insertion type	Lineage	GISAID entries	Other spike mutations	Earliest detection	Latest detection*
I	214:AKKN	ambiguous (codon 215 phase0/I)	B	1	none	Mar 5th, 2020	Mar 5th, 2020
II	214:KLGP	in-frame (codon 215 phase 0)	B.1.177	1	E154K, A222V, D614G	Nov 13th, 2020	Nov 13th, 2020
III	214:AAG	out-of-frame (codon 215 phase I)	A.2.5	1844	L141del, G142del, V143del, D215Y, L452R, D614G	Nov 20th, 2020	Nov 5th, 2021
IV	214:TDR	in-frame (codon 215 phase 0)	B.1.214.2	1228	Q414K, N450K, D614G, T716I	Nov 22nd, 2020	Jun 28th, 2021
V	214:ANRN	ambiguous (codon 215 phase0/I)	γ(P.1)	12	L18F, P26S, D138Y, K417T, E484K, N501Y, D614G, D1139H, V1176F	Dec 23rd, 2020	Apr 5th, 2021
VI	214:KRI	in-frame (codon 215 phase 0)	B	4	V367F, E990A	Dec 28th, 2020	Mar 15th, 2021
VII	214:AQER	ambiguous (codon 215 phase0/I)	ε(B.1.429)	2	S13I, P26S, S98F, W152C, L452R, D614G, T1027I	Jan 15th, 2021	Jan 18th, 2021
VIII	214:DLA	ambiguous (codon 215 phase0/I/II, codon 216 phase 0/I/II)	B.1.2	5	D614G	Jan 17th, 2021	Feb 2nd, 2021
IX	214:QAS	in-frame (codon 215 phase 0)	B.1.639	45	H69del, V70del, Y144del, M153T, T478K, E484K, D614G, T859N, D936Y	Jan 19th, 2021	Nov 4th, 2021
X	216:ADL	ambiguous (codon 216 phase I/II)	B.1.2	1	D614G	Jan 25th, 2021	Jan 25th, 2021
XI	214:DRS	out-of-frame (codon 215 phaseI/II)	B.1	1	D215N, V382L, D614G, M1237I	Feb 1st, 2021	Feb 1st, 2021
XII	214:KFH	in-frame (codon 215 phase 0)	α(B.1.1.7)	3	H69del, V70del, Y144del, N501Y, A570D, D614G, P681H, T716I, S982A, D1118H	Feb 12th, 2021	Feb 22nd, 2021
XIII	214:KAFKQ	in-frame (codon 215 phase 0)	α(B.1.1.7)	2	H69del, V70del, Y144del, A262S, N501Y, A570D, D614G, P681H, T716I, S982A, D1118H	Feb 25th, 2021	Feb 25th, 2021
XIV	214:ER	out-of-frame (codon 215 phase II)	α(B.1.1.7)	1	H69del, V70del, Y144del, D215G, N501Y, A570D, D614G, P681H, I712V, T716I, S982A, D1118H	Mar 11th, 2021	Mar 11th, 2021
XV	214: NWAHW	in-frame (codon 215 phase 0)	B.1.547	1	T19I, T95I, H69del, V70del, D614G, E484A, A879T, T1027I	Mar 22nd, 2021	Mar 22nd, 2021
XVI	214:APR	ambiguous (codon 215 phase0/I)	α(B.1.1.7)	1	H69del, V70del, Y144del, A262S, N501Y, A570D, D614G, P681H, T716I, S982A, D1118H	Mar 31st, 2021	Mar 31st, 2021
XVII	213:KAR	out-of-frame (codon 213 phase II)	B.1.177	1	A222V, A262S, P272L, D614G, P681H, M1229I	Apr 2nd, 2021	Apr 2nd, 2021
XVIII	214:KLRS	ambiguous (codon 215 phase II, codon 216 phase 0)	A.28	6	T76I, D215S, N501T, F592S, H655Y	Apr 23rd, 2021	Jun 22nd, 2021
XIX	214:KGE	in-frame (codon 215 phase 0)	B.1.1.519	1	T732A, T478K, D614G, P681H	Apr 24th, 2021	Apr 24th, 2021
XX	214:W	in-frame (codon 215 phase 0)	B.1	1	T19I, F140del, P139del, L141del, G142del, V143del, Y144del, Y145del, I210del, L242del, A243del, L244del, T470N, S494P, D614G, H655Y, T859N	May 14th, 2021	May 14th, 2021
XXI	216:QMR	out-of-frame (codon 216 phase I)	α(B.1.1.7)	1	L5F, S13I, H69del, V70del, Y144del, D215R, E484K, N501Y, A570D, D614G, P681H, T716I, S982A, D1118H	May 25th, 2021	May 25th, 2021
XXII	214: KLLIRGD	in-frame (codon 215 phase 0)	B.1	2	Q14del, C15del, V16del, N17del, L18del, W64R, T95I, C136Y, N137del, L141del, G142del, V143del, W152R, I210del, G252V, T415A, N440T, E484K, D614G, H655Y, P681H, T859N, Q1011H, G1219C	Jun 4th, 2021	Jun 4th, 2021
XXIII	213:KRLR	out-of-frame (codon 213 phase II)	B.1.1	1	R214Q, D614G, E484D	Jun 6th, 2021	Jun 6th, 2021
XXIV	214:EAR	ambiguous (codon 215 phase I/II/III)	δ(B.1.617.2)	1	T19R, N137del, G142D, E156G, F157del, R158del, L452R, T478K, E484Q, D614G, P681R, D950N	Jun 8th, 2021	Jun 8th, 2021
XXV	214:QCEE	in-frame (codon 215 phase 0)	B.1.247	1	P209S, A222V, T572I	Jul 15th, 2021	Jul 15th, 2021
XXVI	214:ELCD	ambiguous (codon 215 phase I/II/III)	δ(AY.12)	1	T19R, T95I, E156G, F157del, R158del, L452R, T478K, D614G, P681R, D950N	Jul 17th, 2021	Jul 17th, 2022
XXVII	214: NFGGG	in-frame (codon 215 phase 0)	δ(AY.4)	2	T19R, E156G, F157del, R158del, L452R, T478K, D614G, P681R, D950N	Jul 22nd, 2021	Jul 22nd, 2021
XXVIII	214:NES	in-frame (codon 215 phase 0)	δ(AY.16)	1	T19R, G142D, E156G, F157del, R158del, L452R, T478K, D614G, P681R, D950N	Jul 30th, 2021	Jul 30th, 2021
XXIX	214:VPWI	ambiguous (codon 215 phase 0/I)	δ(AY.4)	9	T19R, T95I, G142D, E156G, F157del, R158del, L452R, T478K, D614G, P681R,V622F, D950N	Aug 4th, 2020	Aug 21st, 2021
XXX	214:HSG	in-frame (codon 215 phase 0)	δ(AY.4)	7	T19R, T95I, D138H, G142D, E156G, F157del, R158del, L452R, T478K, D614G, P681R, D950N	Aug 4th, 2021	Aug 25st, 2021
XXXI	214: SYCTKSKC	in-frame (codon 215 phase 0)	η(B.1.525)	1	A67V, H69del, V70del, Y144del, E484K, D614G, A653V, N679del, Q677H, F888L	Aug 5th, 2021	Aug 5th, 2021
XXXII	214:ESH	ambiguous (codon 215 phase 0/I/II)	B.1.240	1	C15F, L141del, G142del, V143del, Y144del, L242del, A243del, L244del, G446V, E484A, D614G, A688V, V1176F	Aug 6th, 2021	Aug 6th, 2021
XXXIII	214:NFG	in-frame (codon 215 phase 0)	δ(AY.25)	3	T19R, S112L, G142D, E156G, F157del, R158del, L452R, T478K, D614G, P681R, D950N	Aug 20th, 2021	Sep 14th, 2021
XXXIV	214:DQAF		δ(B.1.617.2)	1			

Table 1 (*continued*)

		out-of-frame (codon 214 phase II)			T19R, G142D, E156G, F157del, R158del, A222V, V289I, L452R, T478K, D614G, P681R, D950N	Aug 21st, 2021	Aug 21st, 2021
XXXV	214:EGAE	ambiguous (codon 215 phase 0/I/II)	δ(AY.4)	2	T19R, T95I, G142D, E156G, F157del, R158del, L452R, T478K, D614G, P681R, D950N	Sep 2nd, 2021	Sep 2nd, 2021
XXXVI	214:RLR	in-frame (codon 215 phase 0)	δ(AY.3)	2	T19R, G142D, E156G, F157del, R158del, L452R, T478K, D614G, P681R, D950N	Sep 20th, 2021	Sep 20th, 2021
XXXVII	214:GLKG	out-of-frame (codon 215 phase I)	δ(AY.101)	1	T19R, T95I, G142D, E156G, F157del, R158del, L452R, T478K, D614G, P681R, D950N	Oct 1st, 2021	Oct 1st, 2021
XXXVIII	215:EAR	out-of-frame (codon 215 phase II)	δ(AY.4)	1	T19R, T95I, E156G, F157del, R158del, D215N, L452R, T478K, D614G, P681R, D950N	Oct 3rd, 2021	Oct 3rd, 2021
XXXIX	214:RGG	out-of-frame (codon 214 phase II)	δ(AY.100)	2	T19R, T95I, G142D, E156G, F157del, R158del, N394S, D614G, P681R, D950N	Oct 19th, 2021	Nov 8th, 2021
XL	214:VRR	out-of-frame (codon 215 phase I)	δ(AY.113)	1	T19R, G142D, E156G, F157del, R158del, D215H, L452R, D614G, P681R, D950N	Oct 26th, 2021	Oct 26th, 2021
XLI	214:EPE	ambiguous (codon 215 phase 0/I/II)	o (BA.1)	>140,000	A67V, H69del, V70del, T95I, G142D, V143del, Y144del, Y145del, N211del, L212I, G339D, S371L, S373P, S375F, G446S, S477N, T478K, E484A, Q493R, G496S, Q498R, N501Y, Y505H, T547K, D614G, H655Y, P681H, N679K, N764K, N679K, D796Y, N856K, Q954H, N969K, L981F	Nov 8th, 2021	Jan 2nd, 2022
XLII	214:ASPN	out-of-frame (codon 215 phase I)	α(B.1.1.7)	1	H69del, V70del, Y144del, L242del, A243del, L244del, G446V, E484K, Q498K, N501Y, A570D, D614G, P681H, T716I, W886L, S982A, D1118H	Nov 14th, 2021	Nov 14th, 2021
XLIII	215:KGD	ambiguos (codon 215 phase II, codon 216 phase 0)	δ(AY.4.2)	1	T19R, T95I, Y145H, E156G, F157del, R158del, G142D, A222V, L452R, T478K, D614G, P681R, D950N	Nov 18th, 2021	Jan 3rd, 2021
XLIV	213:RWR	out-of-frame (codon 213 phase II)	δ(AY.4)	2	T19R, T95I, G142D, E156G, F157del, R158del, L452R, T478K, D614G, P681R, D950N	Nov 19th, 2021	Nov 22nd, 2021
XLV	215:AGS	out-of-frame (codon 215 phase II)	δ(AY.122)	1	T19R, G142D, E156G, F157del, R158del, L452R, T478K, D614G, P681R, D950N	Nov 29th, 2021	Nov 29th, 2021
XLVI	215:GGD	in-frame (codon 216 phase 0)	δ(AY.25)	5	T19R, G142D, E156G, F157del, R158del, L452R, T478K, D614G, P681R, D950N	Dec 5th, 2021	Dec 7th, 2021
XLVII	214:SRA	in-frame (codon 215 phase 0)	δ(AY.4.2.1)	1	T19R, V36F, T95I, G142D, Y145H, E156G, F157del, R158del, A222V, L452R, T478K, P681R, D614G, D950N	Dec 6th, 2021	Dec 6th, 2021
XLVIII	214:AAVE	out-of-frame (codon 215 phase I)	δ(AY.4)	1	T19R, T95I, G142D, E156G, F157del, R158del, D215N, N282S, L452R, T478K, D614G, P681R, D950N, A1020S	Dec 9th, 2021	Dec 9th, 2021
XLIX	213:SG	in-frame (codon 214 phase 0)	δ(AY.4)	1	T19R, T95I, G142D, E156G, F157del, R158del, L452R, T478K, D614G, P681R, D950N	Dec 16th, 2021	Dec 16th, 2021

[*] as of January 5th, 2022.

associated with at least six independent insertions at RIR1 (insertion XII, XIII, XIV, XVI, XXI and XLII) between February and November 2021 (**Table 1**, **Fig. 2**). A single RIR1 insertion (XXXI) was recorded in August 2021 in the lineage B.1.525 (eta) in the United Kingdom (Ozer et al., 2021) and two genomes characterized by the presence of insertion VII belonging to B.1.429 (epsilon) (Zhang et al., 2021) were sequenced in California in January 2021. Several recently identified insertions at RIR1 are associated with delta (i.e. insertion XXIV, XXVI, XXVII, XXVIII, XXIX, XXX, XXXIII, XXXIV, XXXV, XXXVI, XXVII, XXXVIII, XXXIX, XL, XLIII, XLIV, XLV, XLVI, XLVII, XLVIII and XLIX). None of these have led to significant community spread to date, even though some were linked to small clusters of infections in England (**Table 1**, **Fig. 2**). Albeit not directly linked with variants designated as VOCs or VOIs, other RIR1 insertions were associated with the presence of immunologically relevant spike mutations. This is the case of insertion IX (lineage B.1.639), which is characterized by the contemporary presence of E484K, T478K and by the deletions Δ69/70 (found in RDR1) and Δ144 (found in RDR2), which are shared by several VOCs and VOIs. Curiously, like the omicron insertion XLI, insertions XV, XXI, XXXI, XXXII and XLII also targeted viral genomes carrying both non-synonymous spike mutations at E484 and deletions at RDR1, suggesting a possible role of RIR1 insertions in compensating otherwise slightly deleterious mutations, like previously hypothesized for RDR1 itself (Meng et al., 2021).

Taking into account the limited efforts carried out by several countries in genomic surveillance throughout 2020 and 2021, the insertions reported in **Table 1** and **Fig. 2** may just represent a fraction of those that emerged at RIR1 during the course of the pandemics. Although it was possible to unambiguously ascertain the exact placement of just 34 RIR1 insertions (see **Table 1**), most of them were in-frame, occurring at phase

0 between codons 214 and 215 (17 out of 34 cases, i.e. 50%), between codons 213 and 214 or between codons 215 and 216 (one case each) with no effect on neighboring codons. However, others were out-of-frame, occurring either at phase I (i.e. between the first and the second nucleotide of a codon) or at phase II (i.e. between the second and the third nucleotide of codon) (**Fig. 2**). In detail, three insertions were observed at phase II within codon 213, two at phase II within codon 214, five and four at phase I and II, respectively, within codon 215, and a single one at phase I within codon 216. In such cases, the placement of the insertion often determined a non-synonymous mutation of the residues flanking RIR1 either at the N- or at the C-terminal side (**Table 1**). It is also worth noting that the omicron insertion XLI was associated with a three nucleotides-long, out-of-frame proximal deletion, which affected codons 211 and 212, resulting in the deletion of a single amino acid. Similar deletions are uncommon in other lineages carrying RIR1 insertions, as they have been previously observed in a single other case, i. e. insertion XXII, which displays a Δ210 deletion.

Although the origins of the 49 RIR1 insertions was not investigated in the present study, other authors have previously suggested that they may result from the incorporation either of other regions of the SARS-CoV-2 genome itself, of host mRNAs (Peacock et al., 2021), or of portions of genomic RNA of other endemic coronaviruses co-infecting the host (Venkatakrishnan et al., 2021). These events would be most likely explained by poorly understood copy-choice recombination processes occurring during viral genome replication (Chrisman et al., 2021; Garushyants et al., 2021). Nevertheless, we caution that the short length of RIR1 insertions (usually nine nucleotides) is in most cases not sufficient to unequivocally establish the origins of the inserted nucleotide sequence, since several randomly occurring identical sequence matches

are expected to be found in a broad range of living organisms. On the other hand, when RIR1 insertions are relatively long, such as in the case of the S:ins214GLTSKRN insertion, seemingly acquired in vitro though repeated passages in Vero cell cultures, the robustness of such inferences might be significantly higher (Peacock et al., 2021; Shiliaev et al., 2021).

3.3. Mutational pattern of A.2.5 lineage

As mentioned above, the only two lineages carrying insertions at RIR1 with solid evidence of widespread community transmission before the global emergence of omicron were A.2.5 and B.1.214.2. The inserted amino acid sequence found in A.2.5 is AAG, as the result of the phase I out-of-frame insertion of the nucleotide sequence CGTCAGGCTA within codon 215, which determines the non-synonymous substitution of Asp215 to Tyr (as a result of a GAT->TAT codon replacement) (Table 1, Fig. 2).

Besides the insertion at RIR1, A.2.5 also displays the deletion of three codons (Δ141–143) in RDR2 (Table 1), sometimes extending to codon 144. This region has been previously implicated in antibody escape (McCarthy et al., 2021) and shows deletions in some relevant VOCs and VOIs, including alpha, omicron and eta. In particular, Δ144 appears to largely explain the resistance towards several NTD-directed mAbs displayed by alpha in vitro (P. Wang et al., 2021). Moreover, the insertion at RIR1 is also combined with L452R, a key mutation that confers resistance towards class III RDB-directed antibodies (Greaney et al., 2021), including LY-CoV555, the basis for the formulation of the commercial mAb bamlanivimab developed by Eli Lilly (Starr et al., 2021). Among the lineages currently or previously designated as VOCs and VOIs, L452R is also found in delta, kappa and epsilon. Like the overwhelming majority of the variants circulating in 2021, A.2.5 is characterized by the presence of the prevalent mutation D614G. Although no other spike mutations are widespread in A.2.5, the A.2.5.3 sublineage acquired S477N, shared with omicron and known to strengthen the binding with the ACE2 receptor (Singh et al., 2021). Overall, this

mutation is associated with ~2% of all A.2.5 genomes (Fig. 3A). Other relevant spike non-synonymous mutations, known to significantly alter either ACE2 binding or antibody recognition, were only seldom detected: K417T, N501Y and E484K (which are the hallmark spike mutations of gamma) were simultaneously found in a single genome (EPI_ISL_2, 305,075, see Fig. 3A) sequenced in Texas in May 2021. E484K was found in three additional cases (two in the United States, one in Canada) in April 2021, and N501Y was detected in nine additional cases (eight in the United States, one in Canada) between March and May 2021. Interestingly, in one such cases N501Y was paired with E484Q, which is found in kappa and determines reduced antibody sensitivity, even though not synergistically with L452R (Ferreira et al., 2021). The acquisition of the mutation P681H, known to increase the efficiency of the furin-like cleavage site was documented in 8 cases, 6 of which also displayed N501Y. Such insertions occurred independently in different branches of the A.2.5 evolutionary tree, indicating convergent evolution (see Fig. 3A). Other lineage-defining non-synonymous mutations of A.2.5 are placed in other genomic locations. These included K1657E, F3071Y, T3255I (shared with delta and mu) and H3580Q in ORF1a; P1000L in ORF1b; S74F and G196V in ORF3a; S197L and M234I (shared with iota) in N (see Fig. 3B). The functional consequences of these point mutations are presently unknown.

Root-to-tip genetic distance analysis revealed that the overall nucleotide substitution rate observed in the A.2.5 lineage (and related sublineages) was significantly lower than the average substitution rate computed for SARS-CoV-2 (based on GISAID data), as evidenced by the markedly different slope of the regression line (see Fig. 3C). This was consistent with a substitution rate equal to 4.00×10^{-4} substitutions/site/year, i.e. roughly 12 substitutions/genome/year. Nevertheless, the A.2.5 SARS-CoV-2 genomes detected in the earliest phases of the spread of this lineage (i.e. December 2020) were linked with a number of substitutions significantly higher than the average number of substitutions found in the same period in other SARS-CoV-2 lineages (i.e. ~33 vs ~25).
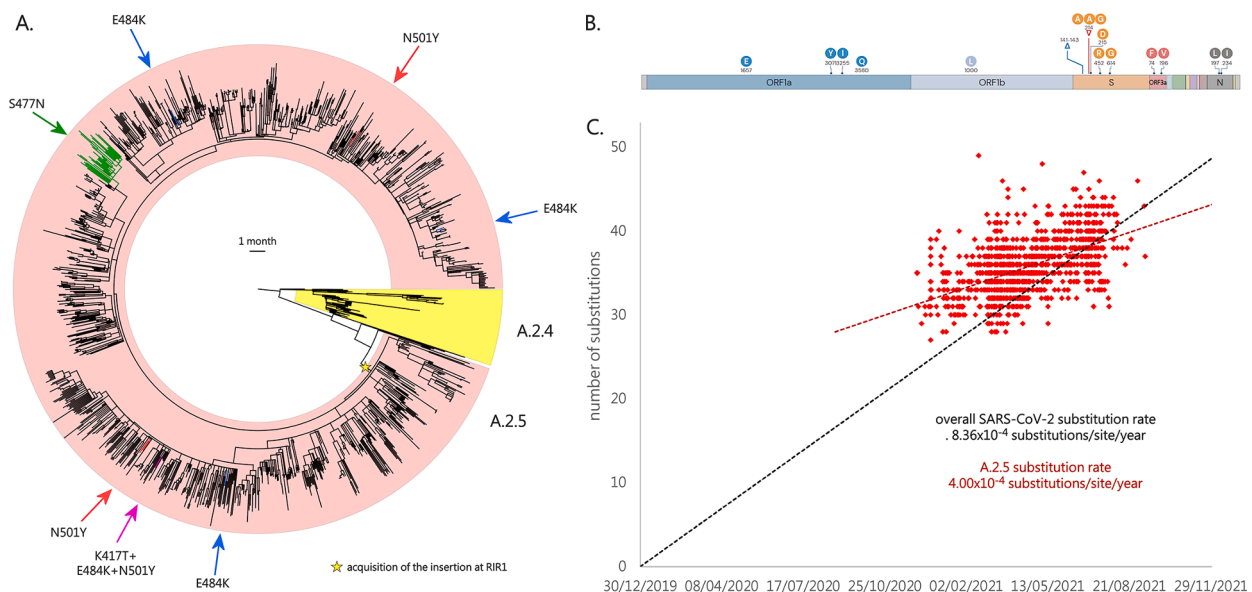

Fig. 3. Panel A: circular time tree exemplifying the phylogeny of the A.2.5 lineage related sublineages. Only high quality, complete genomes have been included. The Wuhan-Hu-1 strain was used to root the tree; the sister lineage A.2.4 is also indicated. The acquisition of relevant spike mutations placed in the receptor binding domain (i.e. S477N, K417T, E484K and N501Y) is marked with arrows. Please note that the monophyletic clade linked with the acquisition of S477N corresponds to the A.2.5.3 sublineage. Panel B: key mutations associated with the A.2. lineages. Genes associated with mutations (compared with the reference strain Wuhan-Hu-1) are indicated; only mutations detected in > 50% of the genomes belonging to this lineage and associated sublineages are shown. Modified from https://outbreak. info/. Panel C: root-to-tip genetic distance (number of nucleotide substitutions) of the genomes belonging to the A.2.5 lineage and related sublineages, compared with the reference genome Wuhan-Hu-1. The black dashed line represents the average rate of mutation of all SARS-CoV-2 sequenced genomes, according to GISAID (i.e. 25 substitutions per genome per year, as of January 5th, 2022). The red dashed line represent the rate of mutation computed for A.2.5. Note that insertions and deletions were excluded from this calculation.

3.4. Emergence and international spread of A.2.5

A.2.5 belongs to one of the very few surviving children lineages of the ancestral lineage A, which, after several months of limited global spread, has led to a few major clusters of infections in 2021, such as the one which involved A.23.1 in Uganda (Bugembe et al., 2021). A.2.5 stems from A.2.4, the dominant lineage in the Panama pandemics during the first half of 2020 (Franco et al., 2020). The first documented cases can be traced back to late November 2020, all within a 100 km² area around the capital city Panamá. However, the precise timing of the emergence of A.2.5, along with the acquisition of insertion III at RIR1 and of the other associated mutations described in the previous section, is presently unclear due to the insufficient molecular surveillance carried out in Central America. To date, less than 1300 out of nearly 500 K covid-19 cases reported in Panama have been selected for viral characterization by sequencing, i.e. less than 0.3% of the total, far below of the threshold that would be sufficient to track emerging variants (Vavrek et al., 2021). The presence of a number of genomes sampled in El Salvador and Guatemala, two countries where genomic surveillance has

been virtually non-existing in 2020, in the earliest-branching clade belonging to A.2.5 (Fig. 3A), leaves the precise geographical origins of this lineage unclear.

Nevertheless, A.2.5 undoubtedly underwent expansion in Panama between December 2020 and February 2021, as revealed by the increase in estimated prevalence from ~60 to ~95%. Interestingly, A.2.5 has been linked with clinically documented reinfections in individuals previously infected by the A.2.4 lineage, which is consistent with the presence of the constellation of non-synonymous spike mutations reported in the previous section, some of which may have immune escape properties (Díaz et al., 2021). The A.2.5 lineage likely spread very early also in the neighboring countries: while investigations carried out in August 2020 failed to identify A.2.5 in Costa Rica (Molina-Mora et al., 2021), the prevalence of this lineage in the country reached 30% between March and June 2021, with the establishment of large clusters of community transmission (Fig. 4). A.2.5 may have undergone a similar spread in other countries in central America, including Belize, Honduras, El Salvador, Guatemala and Mexico, where multiple cases have been detected, starting from the spring of 2021 (Fig. 4).
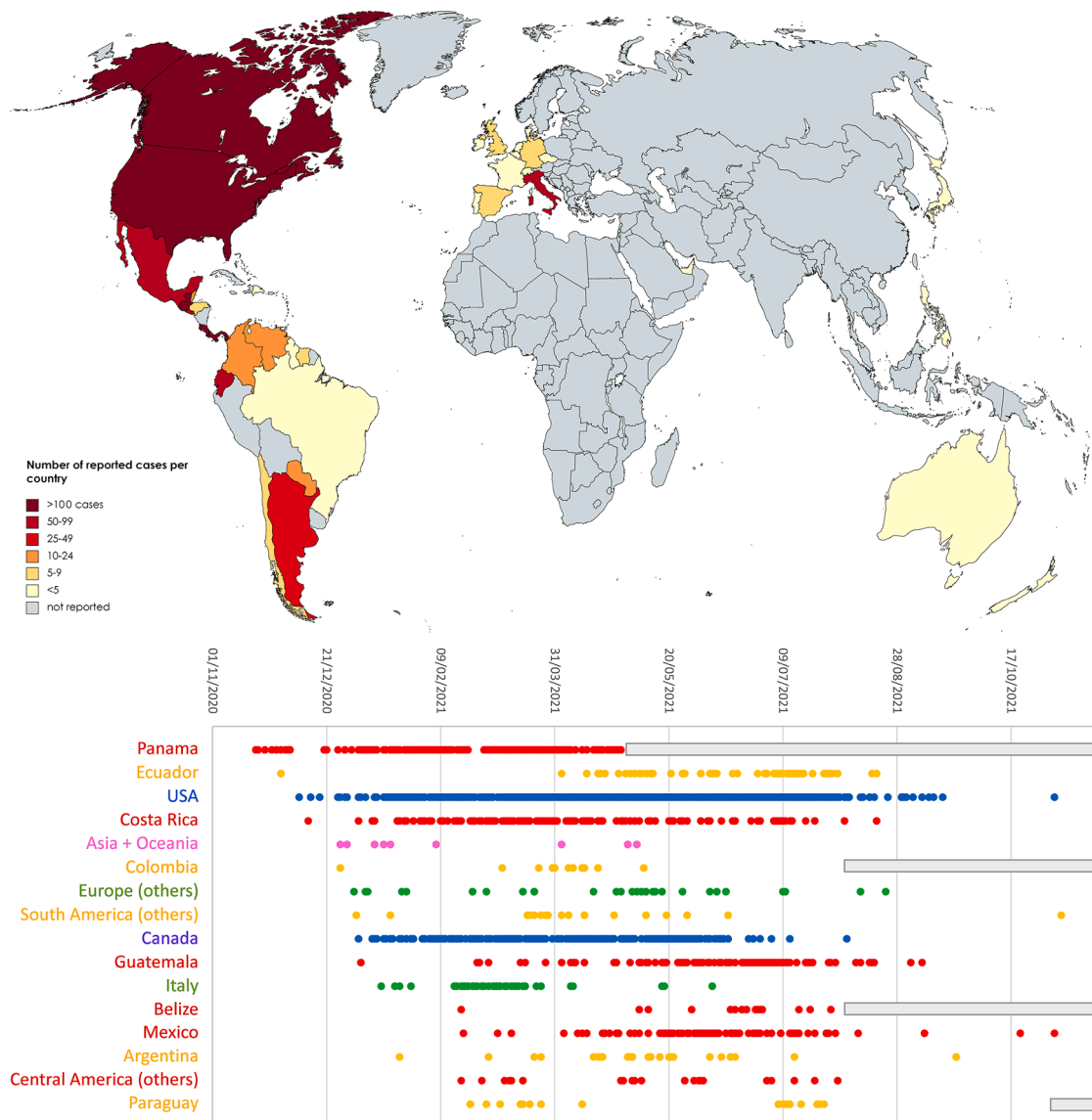

Fig. 4. Upper panel: global spread of A.2.5 and related sublineages. Lower panel: detailed timing of the detection of sequenced genomes belonging to A.2.5 and related sublineages in different countries. Only countries with >= 10 unique days of detection are reported, whereas the others were collapsed in geographic macroareas (i.e. Asia + Oceania, Europe, South America and Central America). The reported dates refer to the dates of sampling reported in GISAID. gray boxes indicate periods of time with no sequencing data available for a given country.

The remarkable spread of SARS-CoV-2 in Central America was connected with a significant number of exported cases, which have sometimes led to clusters of infection abroad. The first evidence of the detection of A.2.5 in southern America dates to December 1st 2020, in Ecuador. In this country, the acquisition of the spike mutation S477N, mentioned in the previous section, later led to the establishment of the A.2.5.3 sublineage (Figs. 3 and 4). Reports in other Latin American countries remain sporadic, but it is worth noting that A.2.5 genomes have been so far sequenced in Argentina, Suriname, Guyana, Grenada, Dominican Republic, Sint Marteen, Cayman Islands, Chile, Colombia, Venezuela, Brazil and Paraguay (Fig. 4). The earliest cases exported in other continents were reported with similar timing in UAE (December 27th, 2020), Philippines (December 30th, 2020) and Australia (January 11th, 2021), which is consistent with the period with the highest incidence of covid-19 infections documented in Panama.

Cases linked with A.2.5 in Europe were identified in Luxembourg, Portugal, Germany, Italy United Kingdom, Czech Republic, France, Belgium, Ireland, Switzerland, Denmark, Netherlands and Spain. In most cases these did not lead to significant community transmission, with the exception of the cluster of cases linked with the A.2.5.2 sublineage recorded in Campania (central Italy) in February-March 2021 (Fig. 4). Similarly, imported cases have most certainly led to local cluster of infections in different areas of the United States and Canada, starting from late 2020 (Fig. 4). Nevertheless, the prevalence of A.2.5 in Northern America never exceeded 0.5%). No SARS-CoV-2 infections linked with A.2.5 have been identified to date in the African continent.

The global frequency of observation of A.2.5 and related sublineages underwent a rapid decline in the second half of 2021, in parallel with the global spread of delta. Just four genomes belonging to this lineage have been sequenced after October 1st, 2021, with the most recent GISAID entry (EPI_ISL_6960593) sampled in Brazil on November 8th, 2021 (Fig. 4). The lack of recent sequencing data from Panama and other countries from Central and Southern America presently does not allow ascertaining whether A.2.5 disappeared in a similar fashion to what occurred for B.1.214.2 during the summer of 2021.

3.5. Impact of RIR1 insertions on the structure of the spike glycoprotein

RIR1 is located in a loop which connects the spike NTD β strands 15 and 16, a region which, unlike most RDRs, does not show any overlap with any known major NTD antigenic sites (Cerutti et al., 2021; McCallum et al., 2021). Hence, the involvement of the insertions reported in this manuscript in antibody escape is unlikely, even though the possibility that this modification may lead to paired structural alterations at distantly related sites, leading to a reduced surface accessibility of canonical antibody epitopes cannot be ruled out. Moreover, the possibility that RIR1 insertions might significantly affect T-cell epitopes remains to be investigated, considering that the majority of T-cell response appears to be directed towards the spike NTD and the S2 subunit (Tarke et al., 2021). Comparative genomics investigations carried out on other viruses belonging to the *Sarbecovirus* subgenus revealed that the RIR1 has been previously prone to structural alterations during the radiation of bat coronaviruses (Garry et al., 2021). In fact, in comparison with the spike proteins of other bat coronaviruses, RmYN02, RacCS203, BANAL-116 and BANAL-247 (Temmam et al., 2021; Zhou et al., 2021, 2020), which are among the closest known relatives to SARS-CoV-2 when genomic recombination is taken into account (Lytras et al., 2021), comprise an insertion of four codons in a position close to RIR1.

Most certainly, the spread of the A.2.5 and B.1.214.2 lineages in different geographical contexts between late 2020 and early 2021, as well as the recent rapid global spread of omicron, indicate that RIR1 insertions are unlikely to have a detrimental impact on the three-dimensional structure of the spike protein or to significantly reduce the infectivity of these variants. At the same time, the well-defined length of the insertions (in the overwhelming majority of cases 3 or 4

codons) suggests that some critical structural constraints, that may prevent the selection of shorter/longer insertions or limit their associated evolutionary benefits, might exist. Several spike mutations located in the NTD can affect the structural organization of the spike protein, altering the stability of the interaction between the RBD and the ACE2 receptor, or its accessibility to antibody recognition. For instance, the NTD Δ69/70 deletion, which, like RIR1, is found in multiple independent lineages, does not determine a significant antibody escape in vitro (P. Wang et al., 2021). However, it is thought to have an important impact on the structure of the spike protein, by compensating otherwise deleterious escape mutations (Meng et al., 2021). In light of these observations, some NTD indels apparently not related with immune escape may act as permissive mutations, by compensating small infectivity deficits associated with other RBD mutations (i.e. L452R in A.2.5, Q414K and N450K in B.1.214.2, N440K, G446S, S477N, T478K, E484A, Q493R, Q498R, N501Y and Y505H in omicron).

Interestingly, the insertion of a seven amino-acid long peptide at RIR1 in SARS-CoV-2 through passages in Vero cell cultures has been recently implicated in enhanced in vitro infectivity, which may be linked with an increase in the positive charge of NTD surface (Shiliaev et al., 2021). According to the authors, this insertion (which is not reported in Table 1 due to its laboratory origin) might have increased the affinity of the spike NTD to heparin, bringing viral particles in close proximity with host cells, thereby favoring the interaction with ACE2. While RIR1 insertions rarely share significant pairwise similarity both at the nucleotide and at the amino acid level (Fig. 2, Table 1), we tested whether the amino acids found in the 49 RIR1 insertions were over-represented compared to expectations (assuming no codon usage bias). As shown in **Supplementary Figure 1**, the basic amino acids arginine and lysine were the most abundant ones (accounting for over 20% of total observations), followed by alanine, glycine and glutamic acid. Overall, lysine was the amino acid characterized by the highest observed/expected ratio (i.e. close to 3) and also arginine showed a moderate increase in frequency compared to expectations, supporting the conclusions by Shiliaev and colleagues about the benefits of acquiring basic residues at RIR1 for viral infectivity. Nevertheless, the two negatively charged residues (i.e. glutamic acid, found in the omicron 214:EPE XLI insertion, and aspartic acid) also had a positive observed/expected ratio, raising the question as to whether such benefits may apply to all charged residues. On the other hand, several amino acids with hydrophobic side chains (e.g. I, M, T, V and Y in particular) were strongly under-represented.

To preliminarily investigate the impact of RIR1 insertions on the structure of the spike protein, we applied molecular dynamics simulations, a well-known technique able to capture and study the dynamical properties of proteins and to assess the effects of mutations, deletions and insertions (Hansson et al., 2002). In this case, we have used a coarse-grained force-field to compare the structural and/or dynamical differences between the spike proteins from the wild-type virus and from the A.2.5 lineage. After 2μs of simulations, the RMSD of the backbone atoms relative to the equivalent initial structures (which represents a global measure of protein fluctuations) was calculated as a function of time to evaluate the stability of MD simulations equilibrium in the two systems. No significant global displacement was detected for any of the two protein models compared with the initial structure, as most of the RMSD values only displayed fluctuations in a range between 0.35 Å and 0.45 Å. Similarly, the presence of a few spike mutations in A.2.5 only led to minor changes in the compactness of the protein, as suggested by the differences of about 1 Å found in the average RYGR values among the two models (**Supplementary Figure 2**). On the other hand, some fluctuations were visible in the RMSF of the A.2.5 spike protein model, in particular in the regions which harbored non-synonymous mutations compared with the wild-type protein.

To understand changes in the direction of motions of the two systems under analysis, PCA was performed on the last 2μs of the simulations, the time after which the systems reached the equilibrium state. The

analysis was then restricted to the backbone beads, as they are less perturbed by statistical noise, providing at the same time a significant characterization of the essential space motions (Michaud-Agrawal et al., 2011). The diagonalization of the covariance matrix of fluctuations of the residues belonging to the backbone resulted in a set of eigenvalues, which were plotted in decreasing order against the corresponding eigenvector indices. The first few eigenvectors corresponded to concerted motions that quickly decreased in amplitude to reach some constrained and more localized fluctuations. Here we present the principal modes along the first eigenvector (Fig. 5A), which covers about 25% of the motions of the protein. Consistently with the placement of non-synonymous mutations (Fig. 3B), this analysis revealed that A.2.5 exhibited some changes in the fluctuations in regions belonging to the NTD and RBD, which are shown in red in Fig. 5B. This indicates that the presence of the mutations and of the insertion at RIR1 may induce local structural and dynamical changes on the spike protein, highlighting the usefulness of performing studies on the dynamical properties of insertions upon their emergence in variants with widespread circulation.

4. Conclusions

The SARS-CoV-2 genome continues to accumulate mutations at a relatively constant rate, occasionally originating new VOCs and VOIs as a result of continued high viral circulation and natural selection. Prior to November 2021, the insertions at RIR1 documented in this work had only led to the emergence of two viral lineages with widespread

transient distribution, i.e. B.1.214.2 and A.2.5, which now appear to be extinct. However, the presence of a RIR1 insertion in the emerging VOC omicron, together with the recurrent independent occurrence of this phenomenon by convergent evolution in multiple viral lineages (including alpha delta), suggests that RIR1 insertions may be linked with an evolutionary advantage, whose magnitude is presently unclear.

In absence of functional data, the role of RIR1 insertions can be only speculated. Based on the lack of overlap with known immune epitopes their involvement in immune escape phenomena appears unlikely, even though their impact on T-cell response remains to be investigated. Similarly, the previously hypothesized role of NTD insertions in enhancing viral infectivity by promoting the interaction with host cell membranes is only partly supported by the over-representation of lysine and arginine residues in RIR1 inserts. On the other hand, we observe a correlation between the presence of RIR1 insertions, RDR deletions and several non-synonymous mutations found in the RBD with known impact on immune evasion, enhanced ACE2 binding and transmissibility. This, together with the predicted impact of RIR1 on the structure of the spike protein, may suggest a possible role as a permissive mutation in compensating otherwise slightly disadvantageous non-synonymous spike RBD mutations. Undoubtedly, our observations strongly suggest that the functional and structural impact of these insertions, with particular focus on omicron, should be the subject of in-depth studies.
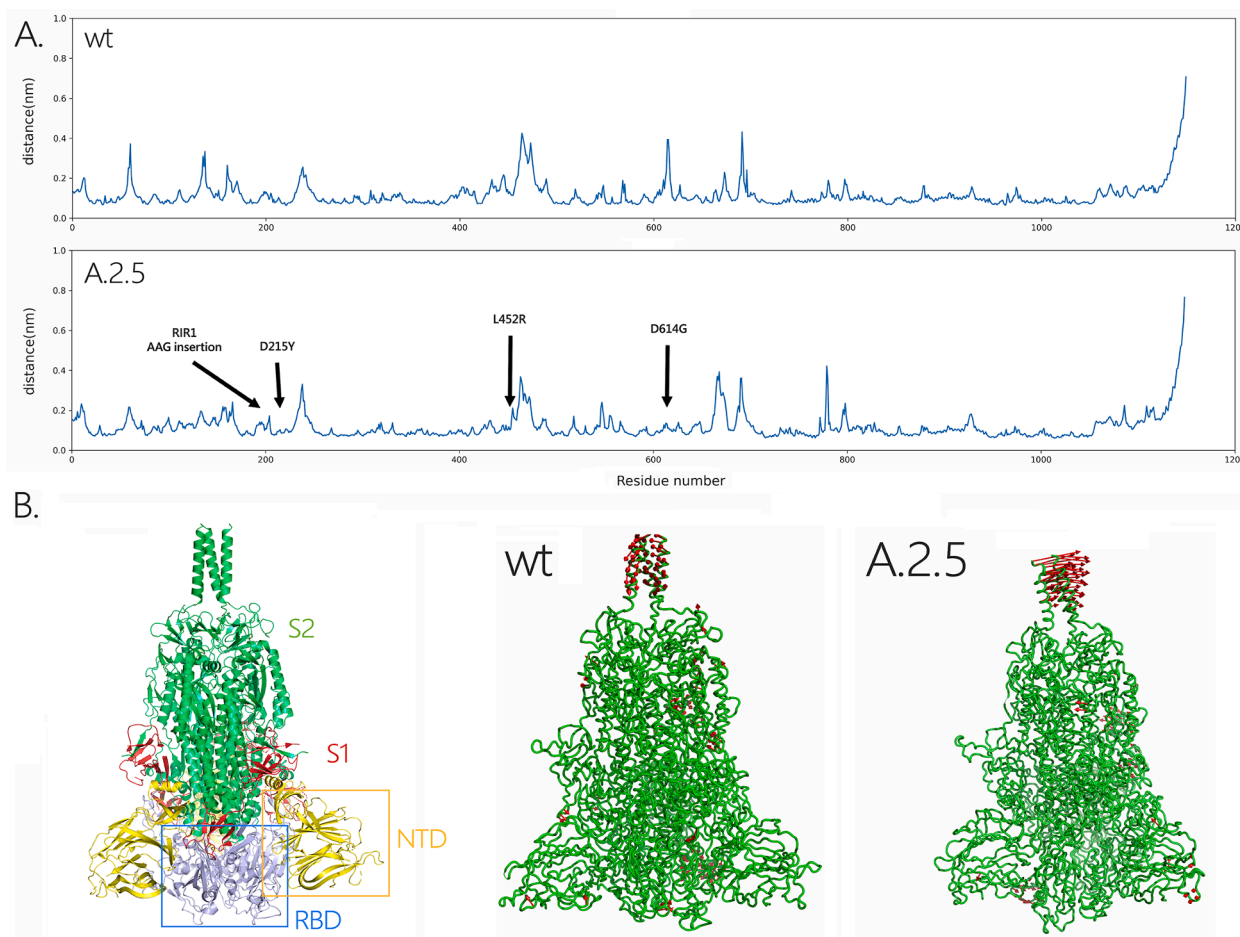

Fig. 5. Panel A: RMSF plot for the models of the wild-type and A.2.5 SARS-CoV-2 spike proteins, with indication of the point and insertion mutations present in the two viral lineages target of his study, compared with the wild type virus. Panel B: Three-dimensional structural models obtained for the wild type and A.2.5 spike proteins. The location of the NTD and RBD (within the S1 subunit) and of the S2 subunit in the spike trimer are shown at the left-hand side. The regions where the most significant fluctuations are marked in red.

CRediT authorship contribution statement

Marco Gerdol: Conceptualization, Data curation, Formal analysis, Investigation, Methodology, Supervision, Visualization, Writing – original draft, Writing – review & editing. **Klevia Dishnica:** Formal analysis, Investigation, Writing – original draft, Writing – review & editing. **Alejandro Giorgetti:** Formal analysis, Investigation, Writing – original draft, Writing – review & editing.

Declaration of Competing Interest

The authors declare they have no competing interests.

Supplementary materials

Supplementary material associated with this article can be found, in the online version, at doi:10.1016/j.virusres.2022.198674.

References

Aguayo-Ortiz, R., Chávez-García, C., Straub, J.E., Dominguez, L., 2017. Characterizing the structural ensemble of γ-secretase using a multiscale molecular dynamics approach. Chem. Sci. 8, 5576–5584. https://doi.org/10.1039/C7SC00980A.

Boni, M.F., Lemey, P., Jiang, X., Lam, T.T.-Y., Perry, .B..W.., Castoe, T.A., Rambaut, A., Robertson, D.L., 2020. Evolutionary origins of the SARS-CoV-2 sarbecovirus lineage responsible for the COVID-19 pandemic. Nat. Microbiol. 5, 1408–1417. https://doi.org/10.1038/s41564-020-0771-4.

Bugembe, D.L., Phan, M.V.T., Ssewanyana, I., Semanda, P., Nansumba, H., Dhaala, B., Nabadda, S., O'Toole, Á.N., Rambaut, A., Kaleebu, P., Cotten, M., 2021. Emergence and spread of a SARS-CoV-2 lineage A variant (A.23.1) with altered spike protein in Uganda. Nat. Microbiol. 6, 1094–1101. https://doi.org/10.1038/s41564-021-00933-9.

Bussi, G., Donadio, D., Parrinello, M., 2007. Canonical sampling through velocity rescaling. J. Chem. Phys. 126, 014101 https://doi.org/10.1063/1.2408420.

Cai, Y., Zhang, J., Xiao, T., Peng, H., Sterling, S.M., Walsh, R.M., Rawson, S., Rits-Volloch, S., Chen, B., 2020. Distinct conformational states of SARS-CoV-2 spike protein. Science 369, 1586–1592. https://doi.org/10.1126/science.abd4251.

Cele, S., Jackson, L., Khoury, D.S., Khan, K., Moyo-Gwete, T., Tegally, H., San, J.E., Cromer, D., Scheepers, C., Amoako, D., Karim, F., Bernstein, M., Lustig, G., Archary, D., Smith, M., Ganga, Y., Jule, Z., Reedoy, K., Hwa, S.-.H., Giandhari, J., Blackburn, J.M., Gosnell, B.I., Karim, S.S.A., Hanekom, W., NGS-SA, Team, C.-K., Gottberg, A. von, Bhiman, J., Lessells, R.J., Moosa, M.-Y.S., Davenport, M.P., Oliveira, T.de, Moore, P.L., Sigal, A., 2021. SARS-CoV-2 Omicron has extensive but incomplete escape of Pfizer BNT162b2 elicited neutralization and requires ACE2 for infection. medRxiv 2021.12.08.21267417. https://doi.org/10.1101/2021.12.08.21267417.

Cerutti, G., Guo, Y., Zhou, T., Gorman, J., Lee, M., Rapp, M., Reddem, E.R., Yu, J., Bahna, F., Bimela, J., Huang, Y., Katsamba, P.S., Liu, L., Nair, M.S., Rawi, R., Olia, A. S., Wang, P., Zhang, B., Chuang, G.-.Y., Ho, D.D., Sheng, Z., Kwong, P.D., Shapiro, L., 2021. Potent SARS-CoV-2 neutralizing antibodies directed against spike N-terminal domain target a single supersite. Cell Host Microbe 29, 819–833. https://doi.org/10.1016/j.chom.2021.03.005 e7.

Choi, B., Choudhary, M.C., Regan, J., Sparks, J.A., Padera, R.F., Qiu, X., Solomon, I.H., Kuo, H.-.H., Boucau, J., Bowman, K., Adhikari, U.D., Winkler, M.L., Mueller, A.A., Hsu, T.Y.-T., Desjardins, M., Baden, L.R., Chan, B.T., Walker, B.D., Lichterfeld, M., Brigl, M., Kwon, D.S., Kanjilal, S., Richardson, E.T., Jonsson, A.H., Alter, G., Barczak, A.K., Hanage, W.P., Yu, X.G., Gaiha, G.D., Seaman, M.S., Cernadas, M., Li, J.Z., 2020. Persistence and Evolution of SARS-CoV-2 in an Immunocompromised Host. N. Engl. J. Med. 383, 2291–2293. https://doi.org/10.1056/NEJMc2031364.

Chrisman, B.S., Paskov, K., Stockham, Nate., Tabatabaei, K., Jung, J.-.Y., Washington, P., Varma, M., Sun, M.W., Maleki, S., Wall, D.P., 2021. Indels in SARS-CoV-2 occur at template-switching hotspots. BioData Min 14, 20. https://doi.org/10.1186/s13040-021-00251-0.

Dagpunar, J., 2021. Interim estimates of increased transmissibility, growth rate, and reproduction number of the Covid-19 B1.617.2 variant of concern in the United Kingdom. medRxiv. https://doi.org/10.1101/2021.06.03.21258293, 2021.06.03.21258293.

Davies, N.G., Abbott, S., Barnard, R.C., Jarvis, C.I., Kucharski, A.J., Munday, J.D., Pearson, C.A.B., Russell, T.W., Tully, D.C., Washburne, A.D., Wenseleers, T., Gimma, A., Waites, W., Wong, K.L.M., van Zandvoort, K., Silverman, J.D., , CMMID COVID-19 Working Group, COVID-19 Genomics UK (COG-UK) Consortium, Diaz-Ordaz, K., Keogh, R., Eggo, R.M., Funk, S., Jit, M., Atkins, K.E., Edmunds, W.J., CMMID COVID-19 Working Group, COVID-19 Genomics UK (COG-UK) Consortium, 2021. Estimated transmissibility and impact of SARS-CoV-2 lineage B.1.1.7 in England. Science 372. https://doi.org/10.1126/science.abg3055 eabg3055.

DeLano, W.L., 2002. Pymol: an open-source molecular graphics tool. CCP4 Newsl. Protein Crystallogr 40, 82–92.

Denison, M.R., Graham, R.L., Donaldson, E.F., Eckerle, L.D., Baric, R.S., 2011. Coronaviruses: an RNA proofreading machine regulates replication fidelity and diversity. RNA Biol 8, 270–279. https://doi.org/10.4161/rna.8.2.15013.

Dhar, M.S., Marwal, R., Vs, R., Ponnusamy, K., Jolly, B., Bhoyar, R.C., Sardana, V., Naushin, S., Rophina, M., Mellan, T.A., Mishra, S., Whittaker, C., Fatihi, S., Datta, M., Singh, P., Sharma, U., Ujjainiya, R., Bhatheja, N., Divakar, M.K., Singh, M. K., Imran, M., Senthivel, V., Maurya, R., Jha, N., Mehta, P., A, V., Sharma, P., Vr, A., Chaudhary, U., Soni, N., Thukral, L., Flaxman, S., Bhatt, S., Pandey, R., Dash, D., Faruq, M., Lall, H., Gogia, H., Madan, P., Kulkarni, S., Chauhan, H., Sengupta, S., Kabra, S., , Indian SARS-CoV-2 Genomics Consortium (INSACOG)‡, Gupta, R.K., Singh, S.K., Agrawal, A., Rakshit, P., Nandicoori, V., Tallapaka, K.B., Sowpati, D.T., Thangaraj, K., Bashyam, M.D., Dalal, A., Sivasubbu, S., Scaria, V., Parida, A., Raghav, S.K., Prasad, P., Sarin, A., Mayor, S., Ramakrishnan, U., Palakodeti, D., Seshasayee, A.S.N., Bhat, M., Shouche, Y., Pillai, A., Dikid, T., Das, S., Maitra, A., Chinnaswamy, S., Biswas, N.K., Desai, A.S., Pattabiraman, C., Manjunatha, M.V., Mani, R.S., Arunachal Udupi, G., Abraham, P., Atul, P.V., Cherian, S.S., Indian SARS-CoV-2 Genomics Consortium (INSACOG)‡, 2021. Genomic characterization and epidemiology of an emerging SARS-CoV-2 variant in Delhi, India. Science 374, 995–999. https://doi.org/10.1126/science.abj9932.

Díaz, Y., Ortiz, A., Weeden, A., Castillo, D., González, C., Moreno, B., Martínez-Montero, M., Castillo, M., Vasquez, G., Sáenz, L., Franco, D., Pitti, Y., Chavarria, O., Gondola, J., Moreno, A.M., Ábrego, L., Beltrán, D., Guerra, I., Chang, J., Chaverra, Z., Guerrero, I., Valoy, A., Gaitán, M., Araúz, D., Morán, E., Chen-Germán, M., Valdespino, E., Rodríguez, R., Corrales, R., Chen-Camaño, R., Pascale, J. M., Martínez, A.A., López-Vergès, S., 2021. SARS-CoV-2 reinfection with a virus harboring mutation in the Spike and the Nucleocapsid proteins in Panama. Int. J. Infect. Dis. 108, 588–591. https://doi.org/10.1016/j.ijid.2021.06.004.

Edgar, R.C., 2004. MUSCLE: multiple sequence alignment with high accuracy and high throughput. Nucleic Acids Res 32, 1792–1797. https://doi.org/10.1093/nar/gkh340.

Ferreira, I.A.T.M., Kemp, S.A., Datir, R., Saito, A., Meng, B., Rakshit, P., Takaori-Kondo, A., Kosugi, Y., Uriu, K., Kimura, I., Shirakawa, K., Abdullahi, A., Agarwal, A., Ozono, S., Tokunaga, K., Sato, K., Gupta, R.K., CITIID-NIHR BioResource COVID-19 Collaboration, Indian SARS-CoV-2 Genomics Consortium, Genotype to Phenotype Japan (G2P-Japan) Consortium, 2021. SARS-CoV-2 B1.617 Mutations L452R and E484Q Are Not Synergistic for Antibody Evasion. J. Infect. Dis. 224, 989–994. https://doi.org/10.1093/infdis/jiab368.

Franco, D., Gonzalez, C., Abrego, L.E., Carrera, J.-.P., Diaz, Y., Caicedo, Y., Moreno, A., Chavarria, O., Gondola, J., Castillo, M., Valdespino, E., Gaitán, M., Martínez-Mandiche, J., Hayer, L., Gonzalez, P., Lange, C., Molto, Y., Mojica, D., Ramos, R., Mastelari, M., Cerezo, L., Moreno, L., Donnelly, C.A., Pascale, J.M., Faria, N.R., Lopez-Verges, S., Martinez, A.A., 2020. Early Transmission Dynamics, Spread, and Genomic Characterization of SARS-CoV-2 in Panama. Emerg. Infect. Dis. 27, 612–615. https://doi.org/10.3201/eid2702.203767.

Garcia-Beltran, W.F., Denis, K.J.S., Hoelzemer, A., Lam, E.C., Nitido, A.D., Sheehan, M.L., Berrios, C., Ofoman, O., Chang, C.C., Hauser, B.M., Feldman, J., Roederer, A.L., Gregory, D.J., Poznansky, M.C., Schmidt, A.G., Iafrate, A.J., Naranbhai, V., Balazs, A. B., 2021. mRNA-based COVID-19 vaccine boosters induce neutralizing immunity against SARS-CoV-2 Omicron variant. Cell. In press. https://doi.org/10.1016/j.cell.2021.12.033.

Garry, R.F., Andersen, K.G., Gallaher, W.R., Tsan-Yuk Lam, T., Gangaparapu, K., Latif, A. A., Beddingfield, B.J., Rambaut, A., Holmes, E.C., 2021. Spike protein mutations in novel SARS-CoV-2 'variants of concern' commonly occur in or near indels. Virological https://virological.org/t/spike-protein-mutations-in-novel-sars-cov-2-variants-of-concern-commonly-occur-in-or-near-indels/605 (accessed 5.5.21).

Garushyants, S.K., Rogozin, I.B., Koonin, E.V., 2021. Template switching and duplications in SARS-CoV-2 genomes give rise to insertion variants that merit monitoring. Commun. Biol. 4, 1–9. https://doi.org/10.1038/s42003-021-02858-9.

Ge, X.-.Y., Wang, N., Zhang, W., Hu, B., Li, B., Zhang, Y.-.Z., Zhou, J.-.H., Luo, C.-.M., Yang, X.-.L., Wu, L.-.J., Wang, J., Wang, B., Zhang, Y., Li, Z.-.X., Shi, .Z..-L., 2016. Coexistence of multiple coronaviruses in several bat colonies in an abandoned mineshaft. Virol. Sin. 31, 31–40. https://doi.org/10.1007/s12250-016-3713-9.

Greaney, A.J., Starr, T.N., Barnes, C.O., Weisblum, Y., Schmidt, F., Caskey, M., Gaebler, C., Cho, A., Agudelo, M., Finkin, S., Wang, Z., Poston, D., Muecksch, F., Hatziioannou, T., Bieniasz, P.D., Robbiani, D.F., Nussenzweig, M.C., Bjorkman, P.J., Bloom, J.D., 2021. Mapping mutations to the SARS-CoV-2 RBD that escape binding by different classes of antibodies. Nat. Commun. 12, 4196. https://doi.org/10.1038/s41467-021-24435-8.

Hansson, T., Oostenbrink, C., van Gunsteren, W., 2002. Molecular dynamics simulations. Curr. Opin. Struct. Biol. 12, 190–196. https://doi.org/10.1016/s0959-440x(02)00308-1.

Harvey, W.T., Carabelli, A.M., Jackson, B., Gupta, R.K., Thomson, E.C., Harrison, E.M., Ludden, C., Reeve, R., Rambaut, A., Peacock, S.J., Robertson, D.L., 2021. SARS-CoV-2 variants, spike mutations and immune escape. Nat. Rev. Microbiol. 19, 409–424. https://doi.org/10.1038/s41579-021-00573-0.

Johnson, B.A., Xie, X., Bailey, A.L., Kalveram, B., Lokugamage, K.G., Muruato, A., Zou, J., Zhang, X., Juelich, T., Smith, J.K., Zhang, L., Bopp, N., Schindewolf, C., Vu, M., Vanderheiden, A., Winkler, E.S., Swetnam, D., Plante, J.A., Aguilar, P., Plante, K.S., Popov, V., Lee, B., Weaver, S.C., Suthar, M.S., Routh, A.L., Ren, P., Ku, Z., An, Z., Debbink, K., Diamond, M.S., Shi, P.-.Y., Freiberg, A.N., Menachery, V.D., 2021. Loss of furin cleavage site attenuates SARS-CoV-2 pathogenesis. Nature 591, 293–299. https://doi.org/10.1038/s41586-021-03237-4.

Katoh, K., Misawa, K., Kuma, K., Miyata, T., 2002. MAFFT: a novel method for rapid multiple sequence alignment based on fast Fourier transform. Nucleic Acids Res 30, 3059–3066. https://doi.org/10.1093/nar/gkf436.

Kistler, K.E., Bedford, T., 2021. Evidence for adaptive evolution in the receptor-binding domain of seasonal coronaviruses OC43 and 229e. eLife 10, e64509. https://doi.org/10.7554/eLife.64509.

Korber, B., Fischer, W.M., Gnanakaran, S., Yoon, H., Theiler, J., Abfalterer, W., Hengartner, N., Giorgi, E.E., Bhattacharya, T., Foley, B., Hastie, K.M., Parker, M.D., Partridge, D.G., Evans, C.M., Freeman, T.M., de Silva, T.I., Angyal, A., Brown, R.L., Carrilero, L., Green, L.R., Groves, D.C., Johnson, K.J., Keeley, A.J., Lindsey, B.B., Parsons, P.J., Raza, M., Rowland-Jones, S., Smith, N., Tucker, R.M., Wang, D., Wyles, M.D., McDanal, C., Perez, L.G., Tang, H., Moon-Walker, A., Whelan, S.P., LaBranche, C.C., Saphire, E.O., Montefiori, D.C., 2020. Tracking Changes in SARS-CoV-2 Spike: evidence that D614G Increases Infectivity of the COVID-19 Virus. Cell 182, 812–827. https://doi.org/10.1016/j.cell.2020.06.043 e19.

Kumar, S., Stecher, G., Li, M., Knyaz, C., Tamura, K., 2018. MEGA X: molecular Evolutionary Genetics Analysis across Computing Platforms. Mol. Biol. Evol. 35, 1547–1549. https://doi.org/10.1093/molbev/msy096.

Laiton-Donato, K., Franco-Muñoz, C., Álvarez-Díaz, D.A., Ruiz-Moreno, H.A., Usme-Ciro, J.A., Prada, D.A., Reales-González, J., Corchuelo, S., Herrera-Sepúlveda, M.T., Naizaque, J., Santamaría, G., Rivera, P., Rojas, P., Ortiz, J.H., Cardona, A., Malo, D., Prieto-Alvarado, F., Gómez, F.R., Wiesner, M., Martínez, M.L.O., Mercado-Reyes, M., 2021. Characterization of the emerging B.1.621 variant of interest of SARS-CoV-2. Infect. Genet. Evol. 95, 105038 https://doi.org/10.1016/j.meegid.2021.105038.

Liu, Z., VanBlargan, L.A., Bloyet, L.-.M., Rothlauf, P.W., Chen, R.E., Stumpf, S., Zhao, H., Errico, J.M., Theel, E.S., Liebeskind, M.J., Alford, B., Buchser, W.J., Ellebedy, A.H., Fremont, D.H., Diamond, M.S., Whelan, S.P.J., 2021. Identification of SARS-CoV-2 spike mutations that attenuate monoclonal and serum antibody neutralization. Cell Host Microbe 29, 477–488. https://doi.org/10.1016/j.chom.2021.01.014 e4.

Lopez Bernal, J., Andrews, N., Gower, C., Gallagher, E., Simmons, R., Thelwall, S., Stowe, J., Tessier, E., Groves, N., Dabrera, G., Myers, R., Campbell, C.N.J., Amirthalingam, G., Edmunds, M., Zambon, M., Brown, K.E., Hopkins, S., Chand, M., Ramsay, M., 2021. Effectiveness of Covid-19 Vaccines against the B.1.617.2 (Delta) Variant. N. Engl. J. Med. 385, 585–594. https://doi.org/10.1056/NEJMoa2108891.

Lustig, Y., Nemet, I., Kliker, L., Zuckerman, N., Yishai, R., Alroy-Preis, S., Mendelson, E., Mandelboim, M., 2021. Neutralizing Response against Variants after SARS-CoV-2 Infection and One Dose of BNT162b2. N. Engl. J. Med. 384, 2453–2454. https://doi.org/10.1056/NEJMc2104036.

Lytras, S., Hughes, J., Martin, D., Klerk, A.de, Lourens, R., Pond, S.L.K., Xia, W., Jiang, X., Robertson, D.L., 2021. Exploring the natural origins of SARS-CoV-2 in the light of recombination. bioRxiv. https://doi.org/10.1101/2021.01.22.427830, 2021.01.22.427830.

Ma, Y., Wu, L., Shaw, N., Gao, Y., Wang, J., Sun, Y., Lou, Z., Yan, L., Zhang, R., Rao, Z., 2015. Structural basis and functional analysis of the SARS coronavirus nsp14–nsp10 complex. Proc. Natl. Acad. Sci. 112, 9436–9441. https://doi.org/10.1073/pnas.1508686112.

Madhi, S.A., Baillie, V., Cutland, C.L., Voysey, M., Koen, A.L., Fairlie, L., Padayachee, S.D., Dheda, K., Barnabas, S.L., Bhorat, Q.E., Briner, C., Kwatra, G., Ahmed, K., Aley, P., Bhikha, S., Bhiman, J.N., Bhorat, A.E., du Plessis, J., Esmail, A., Groenewald, M., Horne, E., Hwa, S.-.H., Jose, A., Lambe, T., Laubscher, M., Malahleha, M., Masenya, M., Masilela, M., McKenzie, S., Molapo, K., Moultrie, A., Oelofse, S., Patel, F., Pillay, S., Rhead, S., Rodel, H., Rossouw, L., Taoushanis, C., Tegally, H., Thombrayil, A., van Eck, S., Wibmer, C.K., Durham, N.M., Kelly, E.J., Villafana, T.L., Gilbert, S., Pollard, A.J., de Oliveira, T., Moore, P.L., Sigal, A., Izu, A., 2021. Efficacy of the ChAdOx1 nCoV-19 Covid-19 Vaccine against the B.1.351 Variant. N. Engl. J. Med. 384, 1885–1898. https://doi.org/10.1056/NEJMoa2102214.

Martonák, R., Laio, A., Parrinello, M., 2003. Predicting crystal structures: the Parrinello-Rahman method revisited. Phys. Rev. Lett. 90, 075503 https://doi.org/10.1103/PhysRevLett.90.075503.

McCallum, M., De Marco, A., Lempp, F.A., Tortorici, M.A., Pinto, D., Walls, A.C., Beltramello, M., Chen, A., Liu, Z., Zatta, F., Zepeda, S., di Iulio, J., Bowen, J.E., Montiel-Ruiz, M., Zhou, J., Rosen, L.E., Bianchi, S., Guarino, B., Fregni, C.S., Abdelnabi, R., Foo, S.-Y.C., Rothlauf, P.W., Bloyet, L.-.M., Benigni, F., Cameroni, E., Neyts, J., Riva, A., Snell, G., Telenti, A., Whelan, S.P.J., Virgin, H.W., Corti, D., Pizzuto, M.S., Veesler, D., 2021. N-terminal domain antigenic mapping reveals a site of vulnerability for SARS-CoV-2. Cell 184, 2332–2347. https://doi.org/10.1016/j.cell.2021.03.028 e16.

McCarthy, K.R., Rennick, L.J., Nambulli, S., Robinson-McCarthy, L.R., Bain, W.G., Haidar, G., Duprex, W.P., 2021. Recurrent deletions in the SARS-CoV-2 spike glycoprotein drive antibody escape. Science 371, 1139–1142. https://doi.org/10.1126/science.abf6950.

Meng, B., Kemp, S.A., Papa, G., Datir, R., Ferreira, I.A.T.M., Marelli, S., Harvey, W.T., Lytras, S., Mohamed, A., Gallo, G., Thakur, N., Collier, D.A., Mlcochova, P., Robson, S.C., Loman, N.J., Connor, T.R., Golubchik, T., Martinez Nunez, R.T., Ludden, C., Corden, S., Johnston, I., Bonsall, D., Smith, C.P., Awan, A.R., Bucca, G., Torok, M.E., Saeed, K., Prieto, J.A., Jackson, D.K., Hamilton, W.L., Snell, L.B., Moore, Catherine, Harrison, E.M., Goncalves, S., Fairley, D.J., Loose, M.W., Watkins, J., Livett, R., Moses, S., Amato, R., Nicholls, S., Bull, M., Smith, D.L., Barrett, Jeff, Aanensen, D.M., Curran, M.D., Parmar, S., Aggarwal, D., Shepherd, J.G., Parker, M.D., Glaysher, S., Bashton, M., Underwood, A.P., Pacchiarini, N., Loveson, K.F., Templeton, K.E., Langford, C.F., Sillitoe, J., de Silva, T.I., Wang, D., Kwiatkowski, D., Rambaut, A., O'Grady, J., Cottrell, S., Holden, M.T.G., Thomson, E.C., Osman, H., Andersson, M., Chauhan, A.J., Hassan-Ibrahim, M.O., Lawniczak, M., Alderton, A., Chand, M., Constantinidou, C., Unnikrishnan, M., Darby, A.C., Hiscox, J.A., Paterson, S., Martincorena, I., Volz, E.M., Page, A.J., Pybus, O.G., Bassett, A.R., Ariani, C.V., Chapman, M.H.S., Li, K.K., Shah, R.N., Jesudason, N.G., Taha, Y., McHugh, M.P., Dewar, R., Jahun, A.S., McMurray, C., Pandey, S., McKenna, J.P., Nelson, A., Young, G.R., McCann, C.M., Elliott, S., Lowe, H., Temperton, B., Roy, S., Price, A., Rey, S., Wyles, M., Rooke, S., Shaaban, S., de Cesare, M., Letchford, L., Silveira, S., Pelosi, E., Wilson-Davies, E., Hosmillo, M., O'Toole, Á., Hesketh, A.R., Stark, R., du Plessis, L., Ruis, C., Adams, H., Bourgeois, Y., Michell, S.L., Gramatopoulos, D., Edgeworth, J., Breuer, J., Todd, J.A., Fraser, C., Buck, D., John, M., Kay, G.L., Palmer, Steve, Peacock, S.J., Heyburn, D., Weldon, D., Robinson, E., McNally, A., Muir, P., Vipond, I.B., Boyes, J., Sivaprakasam, V., Salluja, T., Dervisevic, S., Meader, E.J., Park, N.R., Oliver, K., Jeffries, A.R., Ott, S., da Silva Filipe, A., Simpson, D.A., Williams, Masoli, J.A.H., Knight, B.A., Jones, C.R., Koshy, C., Ash, A., Casey, A., Bosworth, A., Ratcliffe, L., Xu-McCrae, L., Pymont, H.M., Hutchings, S., Berry, Lisa, Jones, K., Halstead, F., Davis, T., Holmes, C., Iturriza-Gomara, M., Lucaci, A.O., Randell, P.A., Cox, A., Madona, P., Harris, K.A., Brown, J.R., Mahungu, T.W., Irish-Tavares, D., Haque, T., Hart, J., Witele, E., Fenton, M.L., Liggett, S., Graham, C., Swindells, E., Collins, J., Eltringham, G., Campbell, S., McClure, P.C., Clark, G., Sloan, T.J., Jones, C., Lynch, J., Warne, B., Leonard, S., Durham, J., Williams, T., Haldenby, S.T., Storey, N., Alikhan, N.-.F., Holmes, N., Moore, Christopher, Carlile, M., Perry, M., Craine, N., Lyons, R.A., Beckett, A.H., Goudarzi, S., Fearn, C., Cook, K., Dent, H., Paul, H., Davies, R., Blane, B., Girgis, S.T., Beale, M.A., Bellis, K.L., Dorman, M.J., Drury, E., Kane, L., Kay, S., McGuigan, S., Nelson, R., Prestwood, L., Rajatileka, S., Batra, R., Williams, R.J., Kristiansen, M., Green, A., Justice, A., Mahanama, A.I.K., Samaraweera, B., Hadjirin, N.F., Quick, J., Poplawski, R., Kermack, L.M., Reynolds, N., Hall, G., Chaudhry, Y., Pinckert, M.L., Georgana, I., Moll, R.J., Thornton, A., Myers, R., Stockton, J., Williams, C.A., Yew, W.C., Trotter, A.J., Trebes, A., MacIntyre-Cockett, G., Birchley, A., Adams, A., Plimmer, A., Gatica-Wilcox, B., McKerr, C., Hilvers, E., Jones, H., Asad, H., Coombes, J., Evans, J.M., Fina, L., Gilbert, L., Graham, L., Cronin, M., Kumziene-Summerhayes, S., Taylor, Sarah, Jones, S., Groves, D.C., Zhang, P., Gallis, M., Louka, S.F., Starinskij, I., Jackson, C., Gourtovaia, M., Tonkin-Hill, G., Lewis, K., Tovar-Corona, J.M., James, K., Baxter, L., Alam, M.T., Orton, R.J., Hughes, J., Vattipally, S., Ragonnet-Cronin, M., Nascimento, F.F., Jorgensen, D., Boyd, O., Geidelberg, L., Zarebski, A.E., Raghwani, J., Kraemer, M.U.G., Southgate, J., Lindsey, B.B., Freeman, T.M., Keatley, J.-.P., Singer, J.B., de Oliveira Martins, L., Yeats, C.A., Abudahab, K., Taylor, B.E.W., Menegazzo, M., Danesh, J., Hogsden, W., Eldirdiri, S., Kenyon, A., Mason, J., Robinson, T.I., Holmes, A., Price, J., Hartley, J.A., Curran, T., Mather, A.E., Shankar, G., Jones, R., Howe, R., Morgan, S., Wastenge, E., Chapman, M.R., Mookerjee, S., Stanley, Rachael, Smith, W., Peto, T., Eyre, D., Crook, D., Vernet, G., Kitchen, C., Gulliver, H., Merrick, I., Guest, M., Munn, R., Bradley, D.T., Wyatt, T., Beaver, C., Foulser, L., Palmer, Sophie, Churcher, C.M., Brooks, E., Smith, K.S., Galai, K., McManus, G.M., Bolt, F., Coll, F., Meadows, L., Attwood, S.W., Davies, A., De Lacy, E., Downing, F., Edwards, S., Scarlett, G.P., Jeremiah, S., Smith, N., Leek, D., Sridhar, S., Forrest, S., Cormie, C., Gill, H.K., Dias, J., Higginson, E.E., Maes, M., Young, J., Wantoch, M., Jamrozy, D., Lo, S., Patel, M., Hill, V., Bewshea, C.M., Ellard, S., Auckland, C., Harrison, I., Bishop, C., Chalker, V., Richter, A., Beggs, A., Best, A., Percival, B., Mirza, J., Megram, O., Mayhew, M., Crawford, L., Ashcroft, F., Moles-Garcia, E., Cumley, N., Hopes, R., Asamaphan, P., Niebel, M.O., Gunson, R.N., Bradley, A., Maclean, A., Mollett, G., Blacow, R., Bird, P., Helmer, T., Fallon, K., Tang, J., Hale, A.D., Macfarlane-Smith, L.R., Harper, K.L., Carden, H., Machin, N.W., Jackson, K.A., Ahmad, S.S.Y., George, R.P., Turtle, L., O'Toole, E., Watts, J., Breen, C., Cowell, A., Alcolea-Medina, A., Charalampous, T., Patel, A., Levett, L.J., Heaney, J., Rowan, A., Taylor, G.P., Shah, D., Atkinson, L., Lee, J.C.D., Westhorpe, A.P., Jannoo, R., Lowe, H.L., Karamani, A., Ensell, L., Chatterton, W., Pusok, M., Dadrah, A., Symmonds, A., Sluga, G., Molnar, Z., Baker, P., Bonner, S., Essex, S., Barton, E., Padgett, D., Scott, G., Greenaway, J., Payne, B.A.I., Burton-Fanning, S., Waugh, S., Raviprakash, V., Sheriff, N., Blakey, V., Williams, L.-.A., Moore, J., Stonehouse, S., Smith, L., Davidson, R.K., Bedford, L., Coupland, L., Wright, V., Chappell, J.G., Tsoleridis, T., Ball, J., Khakh, M., Fleming, V.M., Lister, M.M., Howson-Wells, H.C., Berry, Louise, Boswell, T., Joseph, A., Willingham, I., Duckworth, N., Walsh, S., Wise, E., Moore, N., Mori, M., Cortes, N., Kidd, S., Williams, R., Gifford, L., Bicknell, K., Wyllie, S., Lloyd, A., Impey, R., Malone, C.S., Cogger, B.J., Levene, N., Monaghan, L., Keeley, A.J., Partridge, D.G., Raza, M., Evans, C., Johnson, K., Betteridge, E., Farr, B.W., Goodwin, S., Quail, M.A., Scott, C., Shirley, L., Thurston, S.A.J., Rajan, D., Bronner, I.F., Aigrain, L., Redshaw, N.M., Lensing, S.V., McCarthy, S., Makunin, Alex, Balcazar, C.E., Gallagher, M.D., Williamson, K.A., Stanton, T.D., Michelsen, M.L., Warwick-Dugdale, J., Manley, R., Farbos, A., Harrison, J.W., Sambles, C.M., Studholme, D.J., Lackenby, A., Mbisa, T., Platt, S., Miah, S., Bibby, D., Manso, C., Hubb, J., Dabrera, G., Ramsay, M., Bradshaw, D., Schaefer, U., Groves, N., Gallagher, E., Lee, D., Williams, D., Ellaby, N., Hartman, H., Manesis, N., Patel, V., Ledesma, J., Twohig, K.A., Allara, E., Pearson, C., Cheng, J.K.J., Bridgewater, H.E., Frost, L.R.,

Taylor-Joyce, G., Brown, P.E., Tong, L., Broos, A., Mair, D., Nichols, J., Carmichael, S.N., Smollett, K.L., Nomikou, K., Aranday-Cortes, E., Johnson, N., Nickbakhsh, S., Vamos, E.E., Hughes, R., Rainbow, L., Eccles, R., Nelson, C., Whitehead, M., Gregory, R., Gemmell, M., Wierzbicki, C., Webster, H.J., Fisher, C.L., Signell, A.W., Betancor, G., Wilson, H.D., Nebbia, G., Flaviani, F., Cerda, A.C., Merrill, T.V., Wilson, R.E., Cotic, M., Bayzid, N., Thompson, T., Acheson, E., Rushton, S., O'Brien, S., Baker, D.J., Rudder, S., Aydin, A., Sang, F., Debebe, J., Francois, S., Vasylyeva, T.I., Zamudio, M.E., Gutierrez, B., Marchbank, A., Maksimovic, J., Spellman, K., McCluggage, K., Morgan, M., Beer, R., Afifi, S., Workman, T., Fuller, W., Bresner, C., Angyal, A., Green, L.R., Parsons, P.J., Tucker, R.M., Brown, R., Whiteley, M., Bonfield, J., Puethe, C., Whitwham, A., Liddle, Jennifier, Rowe, W., Siveroni, I., Le-Viet, T., Gaskin, A., Johnson, R., Abnizova, I., Ali, M., Allen, L., Anderson, R., Ariani, C., Austin-Guest, S., Bala, S., Barrett, Jeffrey, Bassett, A., Battleday, K., Beal, J., Beale, M., Bellany, S., Bellerby, T., Bellis, K., Berger, D., Berriman, M., Bevan, P., Binley, S., Bishop, J., Blackburn, K., Boughton, N., Bowker, K., Brendler-Spaeth, T., Bronner, I., Brooklyn, T., Buddenborg, S.K., Bush, R., Caetano, C., Cagan, A., Carter, N., Cartwright, J., Monteiro, T.C., Chapman, L., Chillingworth, T.-.J., Clapham, P., Clark, R., Clarke, A., Clarke, C., Cole, D., Cook, E., Coppola, M., Cornell, L., Cornwell, C., Corton, C., Crackett, A., Cranage, A., Craven, H., Craw, S., Crawford, M., Cutts, T., Dabrowska, M., Davies, M., Dawson, J., Day, C., Densem, A., Dibling, T., Dockree, C., Dodd, D., Dogga, S., Dorman, M., Dougan, G., Dougherty, M., Dove, A., Drummond, L., Dudek, M., Durrant, L., Easthope, E., Eckert, S., Ellis, P., Farr, B., Fenton, M., Ferrero, M., Flack, N., Fordham, H., Forsythe, G., Francis, M., Fraser, A., Freeman, A., Galvin, A., Garcia-Casado, M., Gedny, S., Girgis, S., Glover, J., Gould, O., Gray, A., Gray, E., Griffiths, C., Gu, Y., Guerin, F., Hamilton, W., Hanks, H., Harrison, E., Harrott, A., Harry, E., Harvison, J., Heath, P., Hernandez-Koutoucheva, A., Hobbs, D., Holland, D., Holmes, S., Hornett, G., Hough, N., Huckle, L., Hughes-Hallet, L., Hunter, A., Inglis, S., Iqbal, Z., Jackson, A., Jackson, D., Verdejo, C.J., Jones, M., Kallepally, K., Kay, K., Keatley, J., Keith, A., King, A., Kitchin, L., Kleanthous, M., Klimekova, M., Korlevic, P., Krasheninnkova, K., Lane, G., Langford, C., Laverack, A., Law, K., Lensing, S., Lewis-Wade, A., Liddle, Jennifer, Lin, Q., Lindsay, S., Linsdell, S., Long, R., Lovell, Jamie, Lovell, Jon, Mack, J., Maddison, M., Makunin, Aleksei, Mamun, I., Mansfield, J., Marriott, N., Martin, M., Mayho, M., McClintock, J., McHugh, S., MapcMinn, L., Meadows, C., Mobley, E., Moll, R., Morra, M., Morrow, L., Murie, K., Nash, S., Nathwani, C., Naydenova, P., Neaverson, A., Nerou, E., Nicholson, J., Nimz, T., Noell, G.G., O'Meara, S., Ohan, V., Olney, C., Ormond, D., Oszlanczi, A., Pang, Y.F., Pardubska, B., Park, N., Parmar, A., Patel, G., Payne, M., Peacock, S., Petersen, A., Plowman, D., Preston, T., Quail, M., Rance, R., Rawlings, S., Redshaw, N., Reynolds, J., Reynolds, M., Rice, S., Richardson, M., Roberts, C., Robinson, K., Robinson, M., Robinson, D., Rogers, H., Rojo, E.M., Roopra, D., Rose, M., Rudd, L., Sadri, R., Salmon, N., Saul, D., Schwach, F., Seekings, P., Simms, A., Sinnott, M., Sivadasan, S., Siwek, B., Sizer, D., Skeldon, K., Skelton, J., Slater-Tunstill, J., Sloper, L., Smerdon, N., Smith, Chris, Smith, Christen, Smith, J., Smith, K., Smith, M., Smith, S., Smith, T., Sneade, L., Soria, C.D., Sousa, C., Souster, E., Sparkes, A., Spencer-Chapman, M., Squares, J., Stanley, Robert, Steed, C., Stickland, T., Still, I., Stratton, M., Strickland, M., Swann, A., Swiatkowska, A., Sycamore, N., Swift, E., Symons, E., Szluha, S., Taluy, E., Tao, N., Taylor, K., Taylor, Sam, Thompson, S., Thompson, M., Thomson, M., Thomson, N., Thurston, S., Toombs, D., Topping, B., Tovar-Corona, J., Ungureanu, D., Uphill, J., Urbanova, J., Van, P.J., Vancollie, V., Voak, P., Walker, D., Walker, M., Waller, M., Ward, G., Weatherhogg, C., Webb, N., Wells, A., Wells, E., Westwood, L., Whipp, T., Whiteley, T., Whitton, G., Widaa, S., Williams, M., Wilson, M., Wright, S., Duncan, L. M., Carabelli, A.M., Kenyon, J.C., Lever, A.M., De Marco, A., Saliba, C., Culap, K., Cameroni, E., Matheson, N.J., Piccoli, L., Corti, D., James, L.C., Robertson, D.L., Bailey, D., Gupta, R.K., 2021. Recurrent emergence of SARS-CoV-2 spike deletion H69/V70 and its role in the Alpha variant B.1.1.7. Cell Rep 35, 109292. https://doi. org/10.1016/j.celrep.2021.109292.

Michaud-Agrawal, N., Denning, E.J., Woolf, T.B., Beckstein, O., 2011. MDAnalysis: a toolkit for the analysis of molecular dynamics simulations. J. Comput. Chem. 32, 2319–2327. https://doi.org/10.1002/jcc.21787.

Millet, J.K., Jaimes, J.A., Whittaker, G.R., 2021. Molecular diversity of coronavirus host cell entry receptors. FEMS Microbiol. Rev. 45 https://doi.org/10.1093/femsre/ fuaa057 fuaa057.

Molina-Mora, J.A., Cordero-Laurent, E., Godínez, A., Calderón-Osorno, M., Brenes, H., Soto-Garita, C., Pérez-Corrales, C., , COINGESA-CR Consorcio Interinstitucional de Estudios Genómicos del SARS-CoV-2 Costa Rica, Drexler, J.F., Moreira-Soto, A., Corrales-Aguilar, E., Duarte-Martínez, F., COINGESA-CR Consorcio Interinstitucional de Estudios Genómicos del SARS-CoV-2 Costa Rica, 2021. SARS-CoV-2 genomic surveillance in Costa Rica: evidence of a divergent population and an increased detection of a spike T1117I mutation. Infect. Genet. Evol. J. Mol. Epidemiol. Evol. Genet. Infect. Dis. 92, 104872 https://doi.org/10.1016/j.meegid.2021.104872.

Nelson, G., Buzko, O., Spilman, P., Niazi, K., Rabizadeh, S., Soon-Shiong, P., 2021. Molecular dynamic simulation reveals E484K mutation enhances spike RBD-ACE2 affinity and the combination of E484K, K417N and N501Y mutations (501Y.V2 variant) induces conformational change greater than N501Y mutant alone, potentially resulting in an escape mutant. bioRxiv. https://doi.org/10.1101/ 2021.01.13.426558, 2021.01.13.426558.

Ozer, E.A., Simons, L.M., Adewumi, O.M., Fowotade, A.A., Omoruyi, E.C., Adeniji, J.A., Dean, T.J., Zayas, J., Bhimalli, P.P., Ash, M.K., Godzik, A., Schneider, J.R., Mamede, J.I., Taiwo, B.O., Hultquist, J.F., Lorenzo-Redondo, R., 2021. Coincident rapid expansion of two SARS-CoV-2 lineages with enhanced infectivity in Nigeria. medRxiv. https://doi.org/10.1101/2021.04.09.21255206, 2021.04.09.21255206.

Peacock, T.P., Bauer, D.L., Barcley, W.S., 2021. Putative host origins of RNA insertions in SARS-CoV-2 genomes - SARS-CoV-2 coronavirus. Virological https://virological.org/ t/putative-host-origins-of-rna-insertions-in-sars-cov-2-genomes/761.

Peacock, T.P., Brown, J.C., Zhou, J., Thakur, N., Newman, J., Kugathasan, R., Sukhova, K., Kaforou, M., Bailey, D., Barclay, W.S., 2022. The SARS-CoV-2 variant, Omicron, shows rapid replication in human primary nasal epithelial cultures and efficiently uses the endosomal route of entry. bioRxiv. https://doi.org/10.1101/ 2021.12.31.474653, 2021.12.31.474653.

Planas, D., Veyer, D., Baidaliuk, A., Staropoli, I., Guivel-Benhassine, F., Rajah, M.M., Planchais, C., Porrot, F., Robillard, N., Puech, J., Prot, M., Gallais, F., Gantner, P., Velay, A., Le Guen, J., Kassis-Chikhani, N., Edriss, D., Belec, L., Seve, A., Courtellemont, L., Péré, H., Hocqueloux, L., Fafi-Kremer, S., Prazuck, T., Mouquet, H., Bruel, T., Simon-Lorière, E., Rey, F.A., Schwartz, O., 2021. Reduced sensitivity of SARS-CoV-2 variant Delta to antibody neutralization. Nature 596, 276–280. https://doi.org/10.1038/s41586-021-03777-9.

Price, M.N., Dehal, P.S., Arkin, A.P., 2010. FastTree 2 – Approximately Maximum-Likelihood Trees for Large Alignments. PLoS ONE 5, e9490. https://doi.org/ 10.1371/journal.pone.0009490.

Pulliam, J.R.C., Schalkwyk, C.van, Govender, N., Gottberg, A.von, Cohen, C., Groome, M. J., Dushoff, J., Mlisana, K., Moultrie, H., 2021. Increased risk of SARS-CoV-2 reinfection associated with emergence of the Omicron variant in South Africa. medRxiv. https://doi.org/10.1101/2021.11.11.21266068, 2021.11.11.21266068.

Ren, L., Zhang, Y., Li, J., Xiao, Y., Zhang, J., Wang, Y., Chen, L., Paranhos-Baccalà, G., Wang, J., 2015. Genetic drift of human coronavirus OC43 spike gene during adaptive evolution. Sci. Rep. 5 https://doi.org/10.1038/srep11451.

Ren, W., Qu, X., Li, W., Han, Z., Yu, M., Zhou, P., Zhang, S.-Y., Wang, L.-F., Deng, H., Shi, Z., 2008. Difference in Receptor Usage between Severe Acute Respiratory Syndrome (SARS) Coronavirus and SARS-Like Coronavirus of Bat Origin. J. Virol. 82, 1899–1907. https://doi.org/10.1128/JVI.01085-07.

Resende, P.C., Naveca, F.G., Lins, R.D., Dezordi, F.Z., Ferraz, M.V.F., Moreira, E.G., Coêlho, D.F., Motta, F.C., Paixão, A.C.D., Appolinario, L., Lopes, R.S., Mendonça, A. C., da, F., da Rocha, A.S.B., Nascimento, V., Souza, V., Silva, G., Nascimento, F., Neto, L.G.L., da Silva, F.V., Riediger, I., Debur, M., do, C., Leite, A.B., Mattos, T., da Costa, C.F., Pereira, F.M., dos Santos, C.A., Rovaris, D.B., Fernandes, S.B., Abbud, A., Sacchi, C., Khouri, R., Bernardes, A.F.L., Delatorre, E., Gräf, T., Siqueira, M.M., Bello, G., Wallau, G.L., on behalf of Fiocruz COVID-19 Genomic Surveillance Network, 2021. The ongoing evolution of variants of concern and interest of SARS-CoV-2 in Brazil revealed by convergent indels in the amino (N)-terminal domain of the spike protein. Virus Evol. 7 https://doi.org/10.1093/ve/veab069.

Sabino, E.C., Buss, L.F., Carvalho, M.P.S., Prete, C.A., Crispim, M.A.E., Fraiji, N.A., Pereira, R.H.M., Parag, K.V., Peixoto, P.da S., Kraemer, M.U.G., Oikawa, M.K., Salomon, T., Cucunuba, Z.M., Castro, M.C., Santos, A.A.de S., Nascimento, V.H., Pereira, H.S., Ferguson, N.M., Pybus, O.G., Kucharski, A., Busch, M.P., Dye, C., Faria, N.R., 2021. Resurgence of COVID-19 in Manaus, Brazil, despite high seroprevalence. The Lancet 397, 452–455. https://doi.org/10.1016/S0140-6736 (21)00183-5.

Sagulenko, P., Puller, V., Neher, R.A., 2018. TreeTime: maximum-likelihood phylodynamic analysis. Virus Evol 4. https://doi.org/10.1093/ve/vex042.

Saito, A., Irie, T., Suzuki, R., Maemura, T., Nasser, H., Uriu, K., Kosugi, Y., Shirakawa, K., Sadamasu, K., Kimura, I., Ito, J., Wu, J., Iwatsuki-Horimoto, K., Ito, M., Yamayoshi, S., Loeber, S., Tsuda, M., Wang, L., Ozono, S., Butlertanaka, E.P., Tanaka, Y.L., Shimizu, R., Shimizu, K., Yoshimatsu, K., Kawabata, R., Sakaguchi, T., Tokunaga, K., Yoshida, I., Asakura, H., Nagashima, M., Kazuma, Y., Nomura, K., Horisawa, Y., Yoshimura, K., Takaori-Kondo, A., Imai, M., Tanaka, S., Nakagawa, S., Ikeda, T., Fukuhara, T., Kawaoka, Y., Sato, K., 2021. Enhanced fusogenicity and pathogenicity of SARS-CoV-2 Delta P681R mutation. Nature 1–10. https://doi.org/ 10.1038/s41586-021-04266-9.

Schmidt, F., Muecksch, F., Weisblum, Y., Da Silva, J., Bednarski, E., Cho, A., Wang, Z., Gaebler, C., Caskey, M., Nussenzweig, M.C., Hatziioannou, T., Bieniasz, P.D., 2021. Plasma Neutralization of the SARS-CoV-2 Omicron Variant. N. Engl. J. Med. https:// doi.org/10.1056/NEJMc2119641. In press.

Shen, X., Tang, H., Pajon, R., Smith, G., Glenn, G.M., Shi, W., Korber, B., Montefiori, D.C., 2021. Neutralization of SARS-CoV-2 Variants B.1.429 and B.1.351. N. Engl. J. Med. 384, 2352–2354. https://doi.org/10.1056/NEJMc2103740.

Singh, A., Steinkellner, G., Köchl, K., Gruber, K., Gruber, C.C., 2021. Serine 477 plays a crucial role in the interaction of the SARS-CoV-2 spike protein with the human receptor ACE2. Sci. Rep. 11, 4320 https://doi.org/10.1038/s41598-021-83761-5.

Shiliaev, N., Lukash, T., Palchevska, O., Crossman, D.K., Green, T.J., Crowley, M.R., Frolova, E.I., Frolov, I., 2021. Natural and Recombinant SARS-CoV-2 Isolates Rapidly Evolve In Vitro to Higher Infectivity through More Efficient Binding to Heparan Sulfate and Reduced S1/S2 Cleavage. J. Virol. 95 https://doi.org/10.1128/ JVI.01357-21 e01357-21.

Shu, Y., McCauley, J., 2017. GISAID: global initiative on sharing all influenza data – from vision to reality. Eurosurveillance 22. https://doi.org/10.2807/1560-7917. ES.2017.22.13.30494.

Starr, T.N., Greaney, A.J., Dingens, A.S., Bloom, J.D., 2021. Complete map of SARS-CoV-2 RBD mutations that escape the monoclonal antibody LY-CoV555 and its cocktail with LY-CoV016. Cell Rep. Med. 2 https://doi.org/10.1016/j.xcrm.2021.100255.

Starr, T.N., Greaney, A.J., Hilton, S.K., Ellis, D., Crawford, K.H.D., Dingens, A.S., Navarro, M.J., Bowen, J.E., Tortorici, M.A., Walls, A.C., King, N.P., Veesler, D., Bloom, J.D., 2020. Deep Mutational Scanning of SARS-CoV-2 Receptor Binding Domain Reveals Constraints on Folding and ACE2 Binding. Cell 182, 1295–1310. https://doi.org/10.1016/j.cell.2020.08.012 e20.

Sykes, W., Mhlanga, L., Swanevelder, R., Glatt, T.N., Grebe, E., Coleman, C., Pieterson, N., Cable, R., Welte, A., Berg, K., van den, Vermeulen, M., 2021. Prevalence of anti-SARS-CoV-2 antibodies among blood donors in Northern Cape,

KwaZulu-Natal, Eastern Cape, and Free State provinces of South Africa in January 2021. Research Square. https://doi.org/10.21203/rs.3.rs-233375/v1.

Tarke, A., Sidney, J., Kidd, C.K., Dan, J.M., Ramirez, S.I., Yu, E.D., Mateus, J., da Silva Antunes, R., Moore, E., Rubiro, P., Methot, N., Phillips, E., Mallal, S., Frazier, A., Rawlings, S.A., Greenbaum, J.A., Peters, B., Smith, D.M., Crotty, S., Weiskopf, D., Grifoni, A., Sette, A., 2021. Comprehensive analysis of T cell immunodominance and immunoprevalence of SARS-CoV-2 epitopes in COVID-19 cases. Cell Rep. Med. 2, 100204 https://doi.org/10.1016/j.xcrm.2021.100204.

Temmam, S., Vongphayloth, K., Salazar, E.B., Munier, S., Bonomi, M., Régnault, B., Douangboubpha, B., Karami, Y., Chretien, D., Sanamxay, D., Xayaphet, V., Paphaphanh, P., Lacoste, V., Somlor, S., Lakeomany, K., Phommavanh, N., Pérot, P., Donati, F., Bigot, T., Nilges, M., Rey, F., Werf, S.van der, Brey, P., Eloit, M., 2021. Coronaviruses with a SARS-CoV-2-like receptor-binding domain allowing ACE2-mediated entry into human cells isolated from bats of Indochinese peninsula. Research Square. https://doi.org/10.21203/rs.3.rs-871965/v1.

Teng, S., Sobitan, A., Rhoades, R., Liu, D., Tang, Q., 2021. Systemic effects of missense mutations on SARS-CoV-2 spike glycoprotein stability and receptor-binding affinity. Brief. Bioinform. 22, 1239–1253. https://doi.org/10.1093/bib/bbaa233.

Teruel, N., Mailhot, O., Najmanovich, R.J., 2021. Modelling conformational state dynamics and its role on infection for SARS-CoV-2 Spike protein variants. PLOS Comput. Biol. 17, e1009286 https://doi.org/10.1371/journal.pcbi.1009286.

Van Der Spoel, D., Lindahl, E., Hess, B., Groenhof, G., Mark, A.E., Berendsen, H.J.C., 2005. GROMACS: fast, flexible, and free. J. Comput. Chem. 26, 1701–1718. https://doi.org/10.1002/jcc.20291.

van Dorp, L., Acman, M., Richard, D., Shaw, L.P., Ford, C.E., Ormond, L., Owen, C.J., Pang, J., Tan, C.C.S., Boshier, F.A.T., Ortiz, A.T., Balloux, F., 2020a. Emergence of genomic diversity and recurrent mutations in SARS-CoV-2. Infect. Genet. Evol. 83, 104351 https://doi.org/10.1016/j.meegid.2020.104351.

van Dorp, L., Richard, D., Tan, C.C.S., Shaw, L.P., Acman, M., Balloux, F., 2020b. No evidence for increased transmissibility from recurrent mutations in SARS-CoV-2. Nat. Commun. 11, 1–8. https://doi.org/10.1038/s41467-020-19818-2.

VanInsberghe, D., Neish, A.S., Lowen, A.C., Koelle, K., 2021. Recombinant SARS-CoV-2 genomes circulated at low levels over the first year of the pandemic. Virus Evol 7. https://doi.org/10.1093/ve/veab059.

Vavrek, D., Speroni, S., Curnow, K.J., Oberholzer, M., Moeder, V., Febbo, P.G., 2021. Genomic surveillance at scale is required to detect newly emerging strains at an early timepoint. medRxiv. https://doi.org/10.1101/2021.01.12.21249613, 2021.01.12.21249613.

Venkatakrishnan, A.J., Anand, P., Lenehan, P.J., Suratekar, R., Raghunathan, B., Niesen, M.J.M., Soundararajan, V., 2021. Omicron variant of SARS-CoV-2 harbors a unique insertion mutation of putative viral or human genomic origin. OSF preprints. https://doi.org/10.31219/osf.io/f7txy.

Viana, R., Moyo, S., Amoako, D.G., Tegally, H., Scheepers, C., Althaus, C.L., Anyaneji, U. J., Bester, P.A., Boni, M.F., Chand, M., Choga, W.T., Colquhoun, R., Davids, M., Deforche, K., Doolabh, D., Engelbrecht, S., Everatt, J., Giandhari, J., Giovanetti, M., Hardie, D., Hill, V., Hsiao, N.-.Y., Iranzadeh, A., Ismail, A., Joseph, C., Joseph, R., Koopile, L., Pond, S.L.K., Kraemer, M.U., Kuate-Lere, L., Laguda-Akingba, O., Lesetedi-Mafoko, O., Lessells, R.J., Lockman, S., Lucaci, A.G., Maharaj, A., Mahlangu, B., Maponga, T., Mahlakwane, K., Makatini, Z., Marais, G., Maruapula, D., Masupu, K., Matshaba, M., Mayaphi, S., Mbhele, N., Mbulawa, M.B., Mendes, A., Mlisana, K., Mnguni, A., Mohale, T., Moir, M., Moruisi, K., Mosepele, M., Motsatsi, G., Motswaledi, M.S., Mphoyakgosi, T., Msomi, N., Mwangi, P.N., Naidoo, Y., Ntuli, N., Nyaga, M., Olubayo, L., Pillay, S., Radibe, B., Ramphal, Y., Ramphal, U., San, J.E., Scott, L., Shapiro, R., Singh, L., Smith-Lawrence, P., Stevens, W., Strydom, A., Subramoney, K., Tebeila, N., Tshiabuila, D., Tsui, J., Wyk, S., van, Weaver, S., Wibmer, C.K., Wilkinson, E., Wolter, N., Zarebski, A.E., Zuze, B., Goedhals, D., Preiser, W., Treurnicht, F., Venter, M., Williamson, C., Pybus, O.G., Bhiman, J., Glass, A., Martin, D.P., Rambaut, A., Gaseitsiwe, S., Gottberg, A., von, Oliveira, T.d.e., 2021. Rapid epidemic expansion of the SARS-CoV-2 Omicron variant in southern Africa. medRxiv. https://doi.org/10.1101/2021.12.19.21268028, 2021.12.19.21268028.

Volz, E., Mishra, S., Chand, M., Barrett, J.C., Johnson, R., Geidelberg, L., Hinsley, W.R., Laydon, D.J., Dabrera, G., O'Toole, Á., Amato, R., Ragonnet-Cronin, M., Harrison, I., Jackson, B., Ariani, C.V., Boyd, O., Loman, N.J., McCrone, J.T., Gonçalves, S., Jorgensen, D., Myers, R., Hill, V., Jackson, D.K., Gaythorpe, K., Groves, N., Sillitoe, J., Kwiatkowski, D.P., Flaxman, S., Ratmann, O., Bhatt, S., Hopkins, S., Gandy, A., Rambaut, A., Ferguson, N.M., 2021. Assessing transmissibility of SARS-CoV-2 lineage B.1.1.7 in England. Nature 1–17. https://doi.org/10.1038/s41586-021-03470-x.

Wacharapluesadee, S., Tan, C.W., Maneeorn, P., Duengkae, P., Zhu, F., Joyjinda, Y., Kaewpom, T., Chia, W.N., Ampoot, W., Lim, B.L., Worachotsueptrakun, K., Chen, V. C.-W., Sirichan, N., Ruchisrisarod, C., Rodpan, A., Noradechanon, K., Phaichana, T., Jantarat, N., Thongnumchaima, B., Tu, C., Crameri, G., Stokes, M.M., Hemachudha, T., Wang, .L.-F., 2021. Evidence for SARS-CoV-2 related coronaviruses circulating in bats and pangolins in Southeast Asia. Nat. Commun. 12, 972. https://doi.org/10.1038/s41467-021-21240-1.

Walls, A.C., Park, Y.-.J., Tortorici, M.A., Wall, A., McGuire, A.T., Veesler, D., 2020. Structure, Function, and Antigenicity of the SARS-CoV-2 Spike Glycoprotein. Cell 181, 281–292. https://doi.org/10.1016/j.cell.2020.02.058 e6.

Wang, G.-.L., Wang, Z.-.Y., Duan, L.-.J., Meng, Q.-.C., Jiang, M.-.D., Cao, J., Yao, L., Zhu, K.-.L., Cao, W.-.C., Ma, .M.-.J., 2021a. Susceptibility of Circulating SARS-CoV-2 Variants to Neutralization. N. Engl. J. Med. 384, 2354–2356. https://doi.org/10.1056/NEJMc2103022.

Wang, P., Nair, M.S., Liu, L., Iketani, S., Luo, Y., Guo, Y., Wang, M., Yu, J., Zhang, B., Kwong, P.D., Graham, B.S., Mascola, J.R., Chang, J.Y., Yin, M.T., Sobieszczyk, M., Kyratsous, C.A., Shapiro, L., Sheng, Z., Huang, Y., Ho, D.D., 2021b. Antibody resistance of SARS-CoV-2 variants B.1.351 and B.1.1.7. Nature 1–6. https://doi.org/10.1038/s41586-021-03398-2.

Wang, Z., Schmidt, F., Weisblum, Y., Muecksch, F., Barnes, C.O., Finkin, S., Schaefer-Babajew, D., Cipolla, M., Gaebler, C., Lieberman, J.A., Oliveira, T.Y., Yang, Z., Abernathy, M.E., Huey-Tubman, K.E., Hurley, A., Turroja, M., West, K.A., Gordon, K., Millard, K.G., Ramos, V., Da Silva, J., Xu, J., Colbert, R.A., Patel, R., Dizon, J., Unson-O'Brien, C., Shimeliovich, I., Gazumyan, A., Caskey, M., Bjorkman, P.J., Casellas, R., Hatziioannou, T., Bieniasz, P.D., Nussenzweig, M.C., 2021c. mRNA vaccine-elicited antibodies to SARS-CoV-2 and circulating variants. Nature 592, 616–622. https://doi.org/10.1038/s41586-021-03324-6.

Waterhouse, A., Bertoni, M., Bienert, S., Studer, G., Tauriello, G., Gumienny, R., Heer, F. T., de Beer, T.A.P., Rempfer, C., Bordoli, L., Lepore, R., Schwede, T., 2018. SWISS-MODEL: homology modelling of protein structures and complexes. Nucleic Acids Res 46, W296–W303. https://doi.org/10.1093/nar/gky427.

Willett, B.J., Grove, J., MacLean, O.A., Wilkie, C., Logan, N., Lorenzo, G.D., Furnon, W., Scott, S., Manali, M., Szemiel, A., Ashraf, S., Vink, E., Harvey, W., Davis, C., Orton, R., Hughes, J., Holland, P., Silva, V., Pascall, D., Puxty, K., Filipe, A., da, S., Yebra, G., Shaaban, S., Holden, M.T.G., Pinto, R.M., Gunson, R., Templeton, K., Murcia, P., Patel, A.H., , Investigators, T.C.-19 D.V. (DOVE) C.S., Consortium, T.C.-19G.U. (COG-U., Consortium, T.G.-U.N.V., Investigators, T.E. of V.A.D.C.-19V. (EVADE), Haughney, J., Robertson, D.L., Palmarini, M., Ray, S., Thomson, E.C., 2022. The hyper-transmissible SARS-CoV-2 Omicron variant exhibits significant antigenic change, vaccine escape and a switch in cell entry mechanism. medRxiv. https://doi.org/10.1101/2022.01.03.21268111, 2022.01.03.21268111.

Xie, X., Liu, Y., Liu, J., Zhang, X., Zou, J., Fontes-Garfias, C.R., Xia, H., Swanson, K.A., Cutler, M., Cooper, D., Menachery, V.D., Weaver, S.C., Dormitzer, P.R., Shi, .P.-.Y., 2021. Neutralization of SARS-CoV-2 spike 69/70 deletion, E484K and N501Y variants by BNT162b2 vaccine-elicited sera. Nat. Med. 27, 620–621. https://doi.org/10.1038/s41591-021-01270-4.

Zhang, L., Jackson, C.B., Mou, H., Ojha, A., Peng, H., Quinlan, B.D., Rangarajan, E.S., Pan, A., Vanderheiden, A., Suthar, M.S., Li, W., Izard, T., Rader, C., Farzan, M., Choe, H., 2020. SARS-CoV-2 spike-protein D614G mutation increases virion spike density and infectivity. Nat. Commun. 11, 6013. https://doi.org/10.1038/s41467-020-19808-4.

Zhang, W., Davis, B.D., Chen, S.S., Sincuir Martinez, J.M., Plummer, J.T., Vail, E., 2021. Emergence of a Novel SARS-CoV-2 Variant in Southern California. JAMA 325, 1324–1326. https://doi.org/10.1001/jama.2021.1612.

Zhou, H., Chen, X., Hu, T., Li, J., Song, H., Liu, Y., Wang, P., Liu, D., Yang, J., Holmes, E. C., Hughes, A.C., Bi, Y., Shi, W., 2020. A Novel Bat Coronavirus Closely Related to SARS-CoV-2 Contains Natural Insertions at the S1/S2 Cleavage Site of the Spike Protein. Curr. Biol. 30, 2196–2203. https://doi.org/10.1016/j.cub.2020.05.023 e3.

Zhou, H., Ji, J., Chen, X., Bi, Y., Li, J., Wang, Q., Hu, T., Song, H., Zhao, R., Chen, Y., Cui, M., Zhang, Y., Hughes, A.C., Holmes, E.C., Shi, W., 2021. Identification of novel bat coronaviruses sheds light on the evolutionary origins of SARS-CoV-2 and related viruses. Cell 184, 4380–4391. https://doi.org/10.1016/j.cell.2021.06.008 e14.

Zhu, X., Mannar, D., Srivastava, S.S., Berezuk, A.M., Demers, J.-.P., Saville, J.W., Leopold, K., Li, W., Dimitrov, D.S., Tuttle, K.S., Zhou, S., Chittori, S., Subramaniam, S., 2021. Cryo-electron microscopy structures of the N501Y SARS-CoV-2 spike protein in complex with ACE2 and 2 potent neutralizing antibodies. PLOS Biol. 19, e3001237 https://doi.org/10.1371/journal.pbio.3001237.